atmosphere

Supplementary Materials:

Tara I. Yacovitch [1,*], Brian Lerner [1] , Manjula Canagaratna [1], Conner Daube [1], Robert M. Healy [3], Jonathan M. Wang [3], Edward Fortner [1], Francesca Majluf [1,a], Megan Claflin [1], Joseph R. Roscioli [1], Elizabeth Lunny [1], Scott C. Herndon [1]

S1. Daily Activity Log

The table below summarizes Aerodyne Mobile Laboratory daily activities. This data is reproduced in the accompanying spreadsheet (DailyActivityLogAndSites.xlsx) in the supplemental materials. Latitude and Longitude for each site visited are also available in that spreadsheet.

Table S1. Daily Activity Log and Point Source List. The overall incident wind direction is noted (SW wind means wind from the SW, going towards the NE). Industrial sources visited are listed by their unique ARI_ID.

Date	Broad Categorization	Wind	ARI_ID	Site Description	Point Source Note
2021-05-21	Ozone day/EGLE colocation	SW	Warren Station	EGLE site colocation	
			East 7 Mile	EGLE site colocation	
2021-05-22	Dearborn Loops	W / stagnant		Dearborn Loop	
2021-05-23	Compressor Stations	NW	MA141	Compressor Station	
			MA188	Automaker	
			MA41	Compressor Station	
			MA46	Industrial/Chemical	Null. Nearby gas station
			MA7	Landfill	
			SA157	Compressor Station	
			MA130	Industrial/Chemical	
			MA55	Automaker	No Vocus data
			MA117	Automaker	No Vocus data
2021-05-24	Down Day				
2021-05-25	Terminal Station	SW	WA232	Terminal Station - Downstream Oil and Gas	possible enclosed combustor
				Dearborn Loop	
			WA25	Automaker	Null in most tracers. Try PCBTF. Nearby Power Plant
			WA38	Landfill	
2021-05-26	Automakers and surprise VOCs	SW		Dearborn Loop	Low ambient pressure today - distribution network NG leaks?
			WA137	Automaker	Difficult. Try PCBTF

Date	Broad Categorization	Wind	ARI_ID	Site Description	Point Source Note
			WA27	Automaker	Difficult. Try PCBTF
			WA236	Chemical Waste	
			WA224	Automaker	Null. Nearby WA251 Dominate VOC emissions
			WA251	Steel	
			WA238	Distribution Natural Gas Leak	
			WA124	Industrial/Chemical	
2021-05-27	Chemical Plant and Zug Island	E	WA1/WA8	Steel Manufacturer	Napthalene and benzene. Possible Flare.
			WA58	Industrial/Chemical	Acetone. Tall stack emissions likely not seen. Several stationary points around facility
			WA1/WA8	Steel Manufacturer	Null. part of facility that is south of Zug Island
			WA87/WA0	Automaker/Steel Manufacturer	
			WA18	power plant	same napthalene/benzene signature as zug island coal
2021-05-28	Coordinated River Drive with MECP	NE	WA251/WA252	Tank Farm / Terminal Station - Downstream Oil and Gas	Tank Farm. Other nearby sources
			WA58	Industrial/Chemical	
			WA1/WA8	Steel Manufacturer	
				S-N Transect, Detroit River	Coordinated with MECP mobile lab
				N-S Transect, Detroit River	Coordinated with MECP mobile lab
2021-05-29	Port Huron River Drive, Toluene Source	NE/N	SA96	Industrial/Chemical	
				Sarnia Refineries	
			SA164	Automaker	
			SA37	Paper	Null
				Metal Coatings/Finishing	Uncertain assignment
2021-05-30	Dearborn Loops and Maintenance	NE/SE		Dearborn Loop	
2021-05-31	Down Day	SW			

Date	Broad Categorization	Wind	ARI_ID	Site Description	Point Source Note
2021-06-01	Ozone day/EGLE colocation	SE	East 7 Mile	EGLE site colocation	
			Top of Lake St Clair	Stationary Monitoring	
			New Haven	EGLE site colocation	
2021-06-02	Sarnia	E/SE	MA127	Airport	
			SA157	Compressor Station	
			SA96	Industrial/Chemical	
			Cluster 2	Canadian petrochemical/refinery (Sarnia)	
			Cluster 3	Canadian petrochemical/refinery (Sarnia)	
			WA251/WA252	Tank Farm / Terminal Station - Downstream Oil and Gas	
				Coordinated Drive	
			SA99	Automaker	
			SA50	Industrial/Chemical	quick pass
			WA251/WA252	Terminal Station - Downstream Oil and Gas	No Vocus data
			WA1/WA8	Steel Manufacturer	No Vocus data
			WA247	Dry cleaners	No Vocus data
				Dearborn Loop	No Vocus data
2021-06-03	Conner Creek Automakers	S/SE	WA137/WA27	Automaker	Narrow VOC plume, near rail yard
			WA236	Chemical Waste	Plume propagates to neighborhoods
			WA124	Industrial/Chemical	No Vocus data
2021-06-04	Sterling Heights Automakers	SSW/W	MA154	Metal Coatings/Finishing	No Vocus data
			MA130	Industrial/Chemical	
			MA55	Automaker	
			MA117	Automaker	
			MA198	Automaker	
2021-06-05	Ozone Day	SE	East 7 Mile	EGLE site colocation	
2021-06-06	Ozone Day	SW/SE	East 7 Mile	EGLE site colocation	
			New Haven	EGLE site colocation	

Date	Broad Categorization	Wind	ARI_ID	Site Description	Point Source Note
2022-06-07	Livonia Automakers and Landfill	S		Dearborn Loop	
			WA6	Automaker	
			WA5	Automaker	Acetone, uncorrelated BTEX
			WA17	Landfill	Significant VOC uncorrelated with methane. Fare stack is 30-50 ft high
2021-06-08	Down Day	SE			
2021-06-09	Natural Gas Pipeline Vent and Landfills	SW	WT253	Natural gas pipeline vent	Source is East of nearby Compressor Station.
			WA176	Compressor Station	
			WA17	Landfill	Vocus zero during key VOC area
			WA10	Landfill	CH4 but correlated broad CO, CO2, ethane and HCHO. Separate CO2 plume from the marsh
			MO2	Power Plant	Low level CO/C2H6 correlated. Pretty clean
			MO11	Steel Manufacturer	Mixed with power plant source
			WA58	Industrial/Chemical	Acetone
			WA239	Wastewater treatment plant	
2021-06-10	Port Huron sources and coordinated drive	SE	SA50/SA225	Industrial/Chemical	Not possible to distinguish. SA96 plume is confounding
			SA96	Industrial/Chemical	Got GC hit. Primarily Toluene, also some C3H5O Confounding sources
			SA164	Automaker	
				Coordinated Drive	
			Cluster 2	Canadian petrochemical/refinery (Sarnia)	Got GC. Slight HCHO enhancement and propene in GC. Other Alkanes but little Aromatics

Date	Broad Categorization	Wind	ARI_ID	Site Description	Point Source Note
			Cluster 1	Canadian petrochemical/refinery (Sarnia)	Got GC
			SA3	Power Plant	
			SA3	Power Plant	
			SA31	Compressor Station	
			WA238	Distribution Natural Gas Leak	
2021-06-11	Dearborn & Hospital	E		Dearborn Loop	
			WA238	Distribution Natural Gas Leak	
			WA180	Hospital	
2022-06-12	Down Day	SE			First day with EGLE SO2 monitor
2021-06-13	Dearborn and Woodhaven Sources	NE	WA125	Office building	
			WA163	Terminal Station - Downstream Oil and Gas	
			WA93	Automaker	
			WA232	Terminal Station - Downstream Oil and Gas	
			WA175	Automaker	
			WA241	Waste water treatment plant	
			WA58	Industrial/Chemical	
			WA242	Hospital	
2021-06-14	Oakland County Landfills, Automaker, Hospital	NNW		Dearborn Loop	
			OA20	Landfill	
			OA28	Landfill	
			OA32	Automaker	
			OA233	Industrial/Chemical	
			OA243	Hospital	
2021-06-15	Compressors and Landfills	N	SA15	Power Plant	Vocus maintenance
			SA37	Paper	
			SA165	Compressor Station	very low signal
			SA222	Compressor Station	
			MA141	Compressor Station	
			MA72	Compressor Station	
			MA7	Landfill	
			MA237	Industrial/Chemical	multi VOC

Date	Broad Categorization	Wind	ARI_ID	Site Description	Point Source Note
2021-06-16	Dearborn Loop	NNW		Dearborn Loop	
2022-06-17	Ozone Day - Port Huron	SW	MA237	Industrial/Chemical	
			SA157	Compressor Station	
			Port Huron Armory	Monitoring Station	
2021-06-18	Lincoln Park	SW		Dearborn loop	
			WA250	Metal Recycling	
			WA223	Industrial/Chemical	
			WA244	Industrial/Chemical	
			WA245	Industrial	
			WA212	Terminal Station - Downstream Oil and Gas	
2021-06-19	Ozone Day	NE	Allen Park	EGLE site colocation	
			Oak Park	EGLE site colocation	
			Warren Station	EGLE site colocation	
			MA36	Automaker	
			MA21	Waste water treatment plant	
				HCHO on highway 696	Measured at 42.47718, -83.09242, unknown source
2021-06-20	Automakers and HCHO highway plume	W	WA67	Automaker	
			WA9	Power Plant	
			OA63	Hospital	
				HCHO on highway 696	Measured at UTC 06/20/2021 15:26:44 with position 42.47718, -83.09242
			MA198	Automaker	
			MA196	Automaker	
			MA35	Automaker	
2021-06-21	Down Day and Maintenance	NW			Vocus Fuse change
2021-06-22	Dearborn Sources	SW		Dearborn Loop	
			WA22	Refinery	
			WA0	Steel	
			WA4	Automaker	

Date	Broad Categorization	Wind	ARI_ID	Site Description	Point Source Note
			WA67	Automaker	
2021-06-23	Landfill and Ann Arbor Hospital	S	WA87/WA0	Automaker/Steel Manufacturer	
			WA17	Landfill	
			WT246	Hospital	Isoflurane meas
2021-06-24	Automaker/Steel Manufacturer Facility access and Coordinated Drive	S	WA87	Automaker	
			WA0	Steel Manufacturer	
				Coordinated Drive	
			WA247	Dry cleaners	
2021-06-25	Sterling Heights Automakers and Industrial/Chemical site	SE		Unknown (HCHO)	no enhancement today
			MA46	Concrete and Asphalt	
			MA36	Automaker	
			MA55	Automaker	
			MA155	Automaker	
			MA154	Metal Coatings/Finishing	
			MA127	Airport	no enhancement today
			MA237	Industrial/Chemical	
			WA248	Recycler/Waste	Different signature than WA236
			WA27/WA137	Automakers	
			WA236	Chemical Waste	
2021-06-26	Flooding, power loss	S			AML on generator while parked
2021-06-27	Chemical Waste site with EGLE monitoring	SW	WA143	Airport	
			WA10	Landfill	
			WA140	Power Generation	
			WA236	Chemical waste	EGLE was monitoring on this day
			WA248	Industrial/Chemical	Got GC. limited emissions, see Xylenes, TMB
			WA249	Water Works	
2021-06-28	Dearborn sources and New Haven ozone monitoring	SE		Dearborn Loop	

Date	Broad Categorization	Wind	ARI_ID	Site Description	Point Source Note
			WA1/WA8	Steel Manufacturer	Smelly, site had visible plume
			WA250	Metal Recycling	burning, yellow smoke
			WA193	Industrial/Chemical	
			New Haven	Monitoring Station	
2021-06-29	Refinery site access	SW	WA22	Refinery	Including Stationary GC tank farm sampling

S2. Instrumentation and Methods

The AML was present at the Michigan-Ontario Ozone Source Experiment (MOOSE) in and around Detroit, Michigan, May 20th – June 30th, 2021.

MOOSE data from the Aerodyne Mobile Laboratory (AML) is available on the NASA LARC website at https://www-air.larc.nasa.gov/cgi-bin/ArcView/moose.2021?MOBILE=1

The data is produced in ICARTT file format (https://www.earthdata.nasa.gov/esdis/esco/standards-and-practices/icartt-file-format), and divided by PI.

- **YACOVITCH.TARA**: Aerodyne Mobile Laboratory Gas phase species, position and meteorological parameters

1. Daily Files: 1-hz data, multiple instruments.
2. QAdocument includes instrument details.
3. PlumeNotes included

- **MAJLUF.FRANCESCA**: Aerodyne Research, Inc. Vocus PTR-MS VOCs.

1. Daily Files: 1-hz data, Vocus PTR-MS instrument.
2. QAdocument includes instrument details including comparison of benzene response to GC-EI-ToF benzene

- **LERNER.BRIAN**: Aerodyne Research, Inc. GC-EI-ToF VOCs

1. Single File: 10 minute samples every 30 minutes
2. Instrument details included in the ICARTT header

Data is further archived at the NASA Atmospheric Science Data Center https://asdc.larc.nasa.gov/project/MOOSE (accessed 26 October 2023) under dataset DOI: https://doi.org/10.5067/ASDC/SUBORBITAL/MOOSE/DATA001/Aerodyne-Mobile-Lab_1.

The content of this section includes information from the Quality Assurance documents that accompany the archived datasets at https://www-air.larc.nasa.gov/missions/moose/index.html (accessed 26 October 2023). Please see the data repository for the most up-to-date versions of this information.

S2.1. AMLGAS: Gas phase species, position, and meteorological parameters.

Please direct all questions relating to this dataset to:
Tara Yacovitch, tyacovitch@aerodyne.com
Revised Nov 8, 2021

S2.1.1 General Information

This Quality Assurance Document applies to the ICARTT files with the dataID AMLGAS. An example file is called
MOOSE-AMLGAS_MOBILE_YYYYMMDD_**R2**.ict

Variables are labeled according to ICARTT standards with the format MeasurementCategory_CoreName_MeasurementMode_DescriptiveAttributes

See https://doi.org/10.5067/DOC/ESCO/ESDS-RFC-043v1 (accessed 30 October 2023) for a listing of parameters.

Data was collected on board the Aerodyne Mobile Laboratory [1-3] (AML). The inlet height is approximately 2.8 meters.

Figure S1. The Aerodyne Mobile Laboratory.

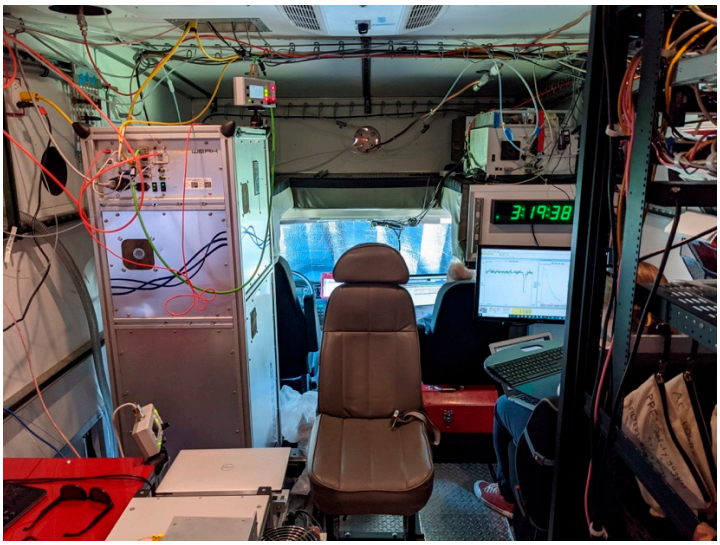

Figure S2. Partial interior view of the Aerodyne mobile laboratory. Clockwise from bottom left corner: the GC-EI-ToF, Vocus PTR-MS, CAPS-NOx and computer infrastructure rack.

Associated Data

Volatile organic hydrocarbon data associated with the Vocus PTR-MS instrument is available under the VocusPTRMS dataID (PI: Francesca Majluf and Jordan Krechmer). Additional VOC data is also available from the gas chromatograph dataID: AMLGC (PI: Brian Lerner).

Time lags

Inlet time corrections (the time it takes for gas to enter the inlet and reach the instrument) have been applied to the data. There is a decent match in time between the various

gas phase instruments (within ~ 1 seconds). When data from 2 different instruments is to be compared or correlated, it will still be necessary to optimize and correct for these small errors in time in order to get the most accurate tracer ratios.

Exhaust and Self-Sampling

This data was collected aboard the Aerodyne Mobile Laboratory (AML) in busy urban areas, often in dense traffic. The collected data will include exhaust measurements, including "self-sampling" periods where the AML sampled its own exhaust. Due to the density of traffic, it was not possible to mark and excise all of these self-sampling periods live. The AML's engine and onboard generators both use diesel fuel. Masks have been created to help identify periods of time unaffected by traffic. See following sections.

The species reported by the AML will allow for an in-depth exploration of vehicular exhaust emissions, and of evaporated fuel, including CO, CO_2, NOx, ethane (C_2H_6) and a slew of compounds measured by the Vocus like BTEX compounds (benzene (C6H7ppb), toluene (C7H9ppb), xylenes + ethylbenzenes (C8H11ppb)), and larger aromatics.

S2.1.2 Time, Position

A unified 1-second time base has been created for each campaign day. Data from various instruments has been interpolated onto this time base.

ICARTT files use elapsed time from midnight UTC. For loading convenience, the Julian day is included in each file Julian Day Lookup Table: https://landweb.modaps.eosdis.nasa.gov/browse/calendar.html (accessed on 23 September 2023). The local time zone in Detroit Michigan was EDT throughout the May-June study. Local time can be calculated as follows: Time_EDT = Time_UTC – 4hrs.

Truck GPS position, heading and speed were logged with a HemiRover V103 GPS compass.

Time and Position Data Description

Table S2. Time and Position Data Description.

Name	Description
Time_Start	Number of seconds elapsed since midnight UTC (Coordinated Universal Time).
julianDay	Day of the year. Day 140 corresponds to May 20th, 2021 UTC.
Latitude	Decimal degrees
Longitude	Decimal degrees
UTM_Easting	Meters east. Horizontal position in Universal Transverse Mercator coordinate system
UTM_Northing	Meters north. Vertical position in Universal Transverse Mercator coordinate system
UTM_Zone	Unitless integer. Universal Transverse Mercator coordinate system zone.
truckHeading	Degrees clockwise from true north. A truck bearing of 90 degrees corresponds to the truck facing due East.
truckSpeed_kmph	Truck speed in kilometers per hour
Elevation_m	Truck elevation in meters above sea level.

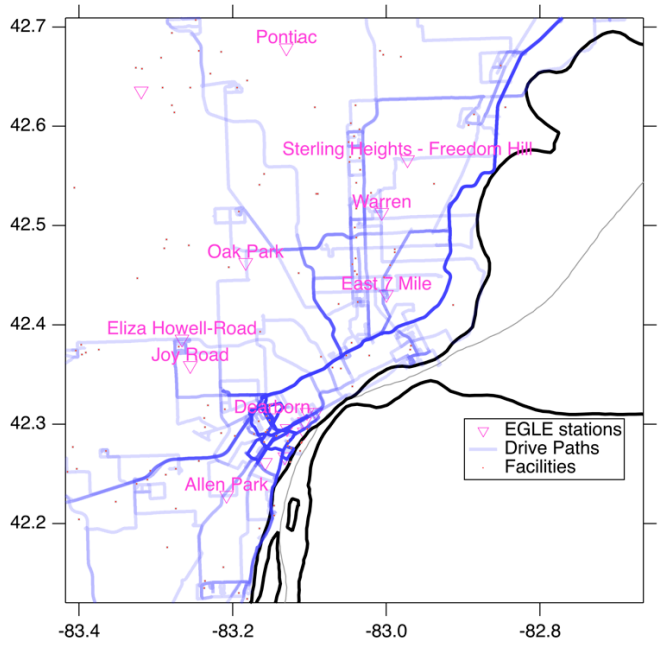

Figure S3. Intermediate scale map showing the AML driven paths. Darker paths indicate more frequent driving on this section.

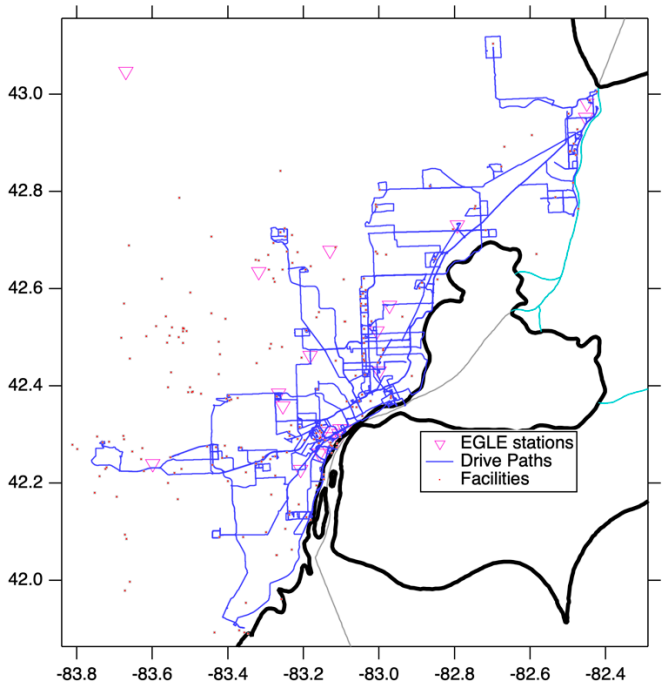

Figure S4. Map showing the full extent of the AML driven paths.

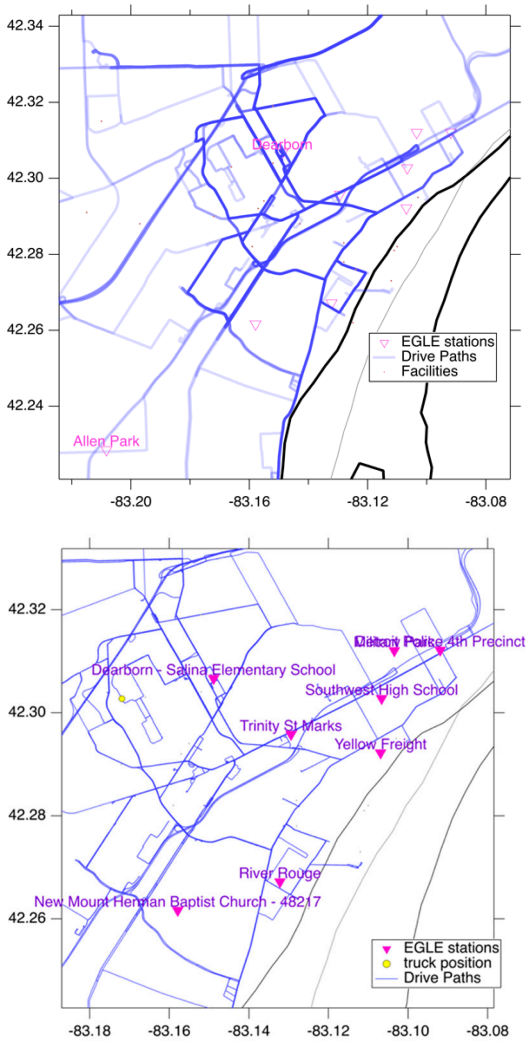

Figure S5. Highlight showing the Dearborn Loop driven paths (**left**) and the EGLE monitoring stations in this area (**right**).

S2.1.3 Mobile Wind

The convention for wind is to plot the incident direction, in degrees clockwise from true north. Wind components in the east and north directions are also included for convenience. This convention means that a wind direction of 45 degrees indicates wind *from* the NE (going *to* the SW).

Raw wind data is at 10 Hz. This fast data is averaged to 1-second using the east and north components, and then the resulting direction and speed calculated.

Replicate wind measurements were collected on the mobile lab (Table S2). The 2D RMYoung ultrasonic anemometer (Model 85004) is the primary reported wind data in the preliminary data. It is mounted to the top of the truck roof. Legal limits to the AML height prevent lofting this anemometer any further up, and so wind data at high speeds are impacted by the body of the truck and are not accurate.

At 6/25/21 15:37:59 UTC, there was a sudden change in RMYoung 2D anemometer rotation, as indicated by apparent wind readings of 41.1 degrees while driving on the highway. Prior to this event, apparent wind is around 0 when driving at high speeds when wind speeds are low. This time coincides with a glitch in wind speed (see Figure S6). The rotation is corroborated by comparison with stationary wind data from EGLE at the Dearborn station (purple traces). The most likely explanation is that the unit was rotated by a

low-hanging branch. Data after this event has been rotated by 41.1 degrees (red trace); data prior to this event maintains a rotation of 0.

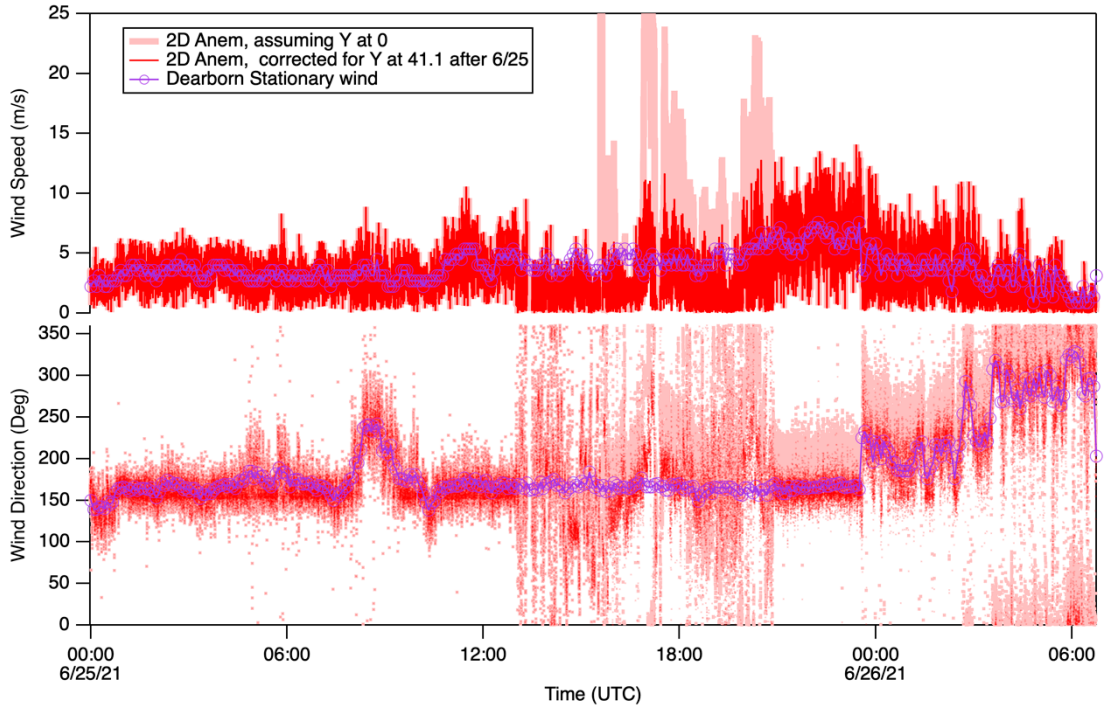

Figure S6. Detail of 2D RMYoung measurements showing a glitch and sudden rotation of the unit. The truck was mobile and off-site from ~1:00 – 21:00 UTC.

Two additional wind measurements were taken. They are not reported and are used for QA only. The 3D RMYoung ultrasonic anemometer (Model 81000RE) is mounted to the truck inlet pole (this anemometer is mounted below the height of the truck body, again due to restrictions on safe vehicle height). For this reason, 3D winds from the truck rear are not accurately measured. An Airmar 200WX is also mounted to the truck roofline and provides redundant GPS and wind data.

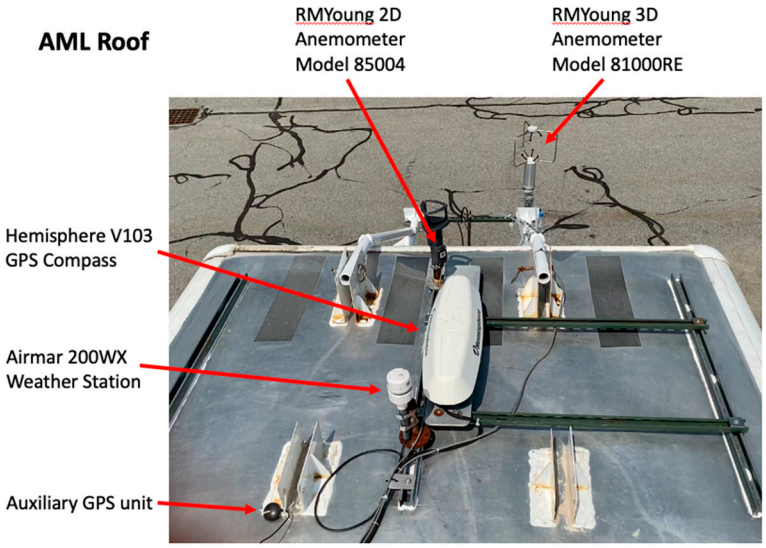

Figure S7. AML Roofline during MOOSE 2021. In this picture the 2D anemometer is rotated 41.1 deg. off axis (counterclockwise).

Wind Data Description

Table S3. Wind data description.

Name	Description
wind_E_metersPerSecond	Incident wind component from the east in meters per second. Measured with the RMYoung 2D ultrasonic anemometer (model 85004) and corrected for truck heading and speed.
wind_N_metersPerSecond	Incident wind component from the north, in meters per second. Measured with the RMYoung 2D ultrasonic anemometer (model 85004) and corrected for truck heading and speed.
wind_dir_degrees	Incident wind direction, in degrees clockwise from true north. Measured with the RMYoung 2D ultrasonic anemometer (model 85004) and corrected for truck heading and speed.
wind_speed_MetersPerSecond	Wind speed, in meters per second. Measured with the RMYoung 2D ultrasonic anemometer (model 85004) and corrected for truck heading and speed.
Temperature_C	Degrees C. Outdoor temperature measured with the RMYoung 3D ultrasonic anemometer (Model 81000RE)
Solar_arbUnits	Insolation, in arbitrary units. This is measured by the ARISense small sensor mounted to the truck roofline. A power outage on 6/26/2021 caused this unit to fail.

S2.1.4 Gas Phase Species

Four Tunable Infrared Laser Direct Absorption Spectrometers (TILDAS) [4] made by Aerodyne Research, Inc. were used during MOOSE. Three single-laser TILDAS-CS measured 1) CO, N_2O, H_2O; 2) HCHO and HCOOH [5]; 3) CH_4 and C_2H_6 [6]. All 3 of these instruments used 76 m multipass cells. A dual-laser TILDAS-FD with 200 m cell was used to measure NO and NO_2. A Licor 6262 non-dispersive infrared (NDIR) was used to measure CO_2, and a 254 nm 2BTech Model 205 Ozone monitor for O_3. An Aerodyne CAPS-NO_2 equipped with an ozonator for conversion of all NOx to NO_2. This yielded a measure of total NOx (the sum of NO and NO_2). A secondary 2BTech ozone monitor (data not reported) was available for backup ambient O_3 and to intermittently check the ozonator functionality. SO_2 was measured for the second half of the campaign using a Teledyne API Model T100 UV Fluorescence SO_2 Analyzer owned by EGLE.

TILDAS instruments rely on the HITRAN database of spectral lines. For most uncalibrated TILDAS species, we expect concentrations to be biased slightly low, and to be within 5-10% of reported. When available, calibrations have been applied. Preliminary calibrations for field data have been applied when available. These calibration factors are listed in the table below.

During the campaign, ultra-zero air was delivered to the gas phase inlet every 15 minutes in excess of the inlet flow. There are two types of zero corrections that can be done. 1) Spectral backgrounding refers to the TILDAS instrument backgrounding procedure where analyte-free air is delivered in excess of instrument flow, and a "background" spectrum is collected. This spectrum is then used to subtract out optical artifacts from the data. 2) Zero corrections refer to offset corrections that are done after data acquisition for the ozone and CO_2 instruments.

Gas Phase Species Data Description

The table below summarizes the gas phase data reported under the AMLGAS data ID. Additional instrument notes are included after the table.

Table S4. Gas phase data reported under the AMLGAS data ID.

Name	Description	Calibration Factor Applied (Final_Data = Raw_data/cal)
O3_ppb	Ozone (O_3) in parts-per-billion (ppb). Zero-corrected and calibrated using a Echotech Serinus O_3 and NO_2 Dilution Calibrator.	1.009
CH4_ppb	Methane (CH_4) in parts-per-billion (ppb). This is a dry air mixing ratio. Spectrally backgrounded and calibrated.	0.927
C2H6_ppb	Ethane (C_2H_6) in parts-per-billion (ppb). This is a dry air mixing ratio. Spectrally backgrounded and calibrated.	0.851
CO2_ppm	Carbon dioxide mixing ratio in parts-per-million (ppm). Zero-corrected and calibrated.	1.183
CO_ppb	Carbon monoxide mixing ratio in parts-per-billion (ppb). This is an ambient air mixing ratio. Un-zeroed due to known presence of CO in ultra-zero-air tanks. Calibrated.	1.064
N2O_ppb	Nitrous oxide (N_2O) concentration in parts-per-billion. This is an ambient air mixing ratio. Zeroes checked but no correction needed. Calibrated.	0.988
H2O_ppb	Water vapor (H_2O) concentration in parts-per-billion (ppb). Ambient air mixing ratio. Uncalibrated.	-
HCHO_ppb	Formaldehyde (HCHO). This is a dry air mixing ratio. Spectrally backgrounded. No direct calibration available. See comparison with this instrument's measure of H_2O for an estimate of the bias.	-
HCOOH_ppb	Formic acid (HCOOH). This is a dry air mixing ratio. Spectrally backgrounded. No calibration available.	-
NO_ppb	Nitric Oxide (NO). This is an ambient air mixing ratio. Spectrally backgrounded. Calibration applied but is expected to change after post-campaign calibrations.	0.865
NO2_ppb	Nitrogen dioxide (NO_2). This is an ambient air mixing ratio. Spectrally backgrounded. Calibration applied but is expected to change after post-campaign calibrations.	0.860 & 0.867 (see note)
NOx_ppb	Total NOx. This is an independent measurement of NOx separate from the NO and NO_2 measurements above. Dry-air mixing ratio. Zeroed and calibrated.	1.114
SO2_ppb	Sulfur dioxide mixing ratio in parts-per-billion (ppb). No Calibration or correction	-

S2.1.5 General QA notes

There are a few data gaps affecting multiple instruments. A gap on 6/5/2021 (~23 hours) was due to a breaker issue in the mobile lab. A gap on 6/26/2021 (~6 hrs) was due to a power outage at the site due to regional flooding. The AML ran on generator

overnight until power was restored. After 6/30/2021 12:30 there was a break in the inlet line from removal of the SO_2 monitor, and no data on this inlet is reported.

Ambient vs Dry air mixing ratios

Certain data are reported as ambient air mixing ratios or ambient mole fraction (AMF). For comparison with other datasets, it is often useful to use dry air mixing ratios or dry mole fraction (DMF), which is corrected for the dilution effect of water vapor in a sample. To calculate dry air mixing ratio (C_s^{dry}) from the ambient air mixing ratio (C_s^{wet}), convert using the formula below, using the water trace H_2O_ppb from the CO-N_2O TILDAS.

$$C_S^{dry}[ppb] = \frac{C_S^{wet}}{1-\frac{n_{water}}{n_{tot}}} = \frac{C_S^{wet}}{1-C_{water}^{wet}} = \frac{C_S^{wet}[ppb]}{1-C_{water}^{wet}[\%]\cdot 10^{-2}} = \frac{C_S^{wet}[ppb]}{1-C_{water}^{wet}[ppb]\cdot 10^{-9}} \quad (1)$$

O3_ppb

The ozone trace is a 2-second dataset that has been interpolated onto the 1-second unified time base. Occasionally, rapid spikes in O_3 without concomitant reductions in NOx were observed while stationary at Dearborn. They are observed in both AML O_3 instruments and also in the EGLE monitoring station data. These spikes have been excised from the data. We hypothesize that they are due to an interferer in the UV.

This instrument's internal scrubbers were changed prior to the campaign and resulted in an excellent measurement even during intense VOC plumes from aromatic species expected to interfere with O_3.

A calibration factor of 1.009 was applied (divided). This is the average of two calibration factors pre- and post- campaign which were 16% different. Between these two calibration points, the Echotech calibrator was sent in for recalibration, but a comparison of new/old Echotech cal factors does not explain the difference. Past experience with the 2BTech unit does not lead us to believe its calibration would have drifted systematically throughout the campaign, and so a single average calibration factor was applied.

HCHO_ppb and HCOOH_ppb

Dry air mixing ratios in parts-per-billion (ppb). Formaldehyde (HCHO) and formic acid (HCOOH) are measured between 1764.1 and 1765.5 cm^{-1}. The TILDAS-CS that measures HCHO and HCOOH also measures H_2O (unreported).

Spectral refits were done for 5/20 18:00 - 5/21/13:00 and from 6/9 to 6/21. The purpose was to fix a failed or fixed frequency lock on the strong water line.

The water measurement from this instrument was compared to the reported water measurement from the TILDAS-CS-N_2O-CO, yielding a slope of 0.986 ppb/ppb. This means that the water line from this instrument is biased 1.4% low versus the primary water measurement. The HITRAN database reports line intensity uncertainties between 5-10% for H_2O at 1764.699 cm^{-1}; 5-10% for HCHO; and 10-20% for HCOOH. We do not correct or calibrate HCHO or HCOOH since the water comparison is within the uncertainties of the HITRAN lines, and the calibration of the CO-N_2O TILDAS is good.

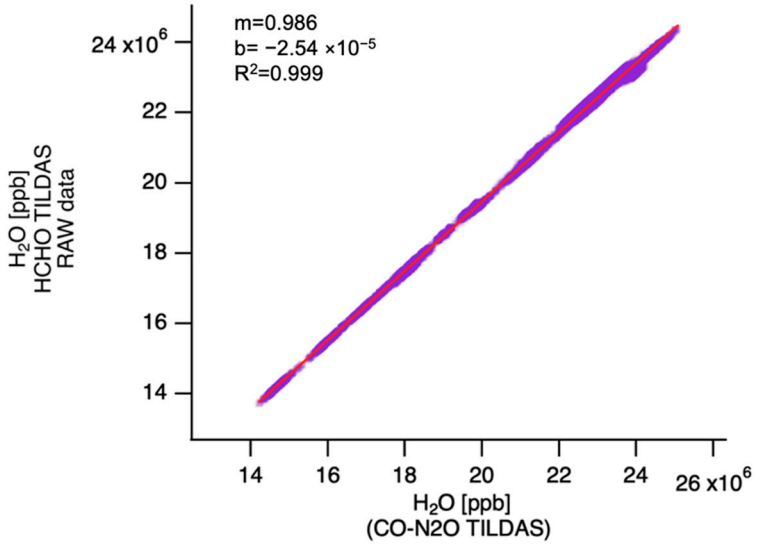

Figure S8. Comparison of water line from the HCHO TILDAS to the water line from the CO-N_2O TILDAS. Zeroes contain residual water, so this comparison uses the un-backgrounded spectral data present in the RAW data files.

HCHO data is also available at several EGLE monitoring stations, including those in the Dearborn area which were routinely visited during the campaign.

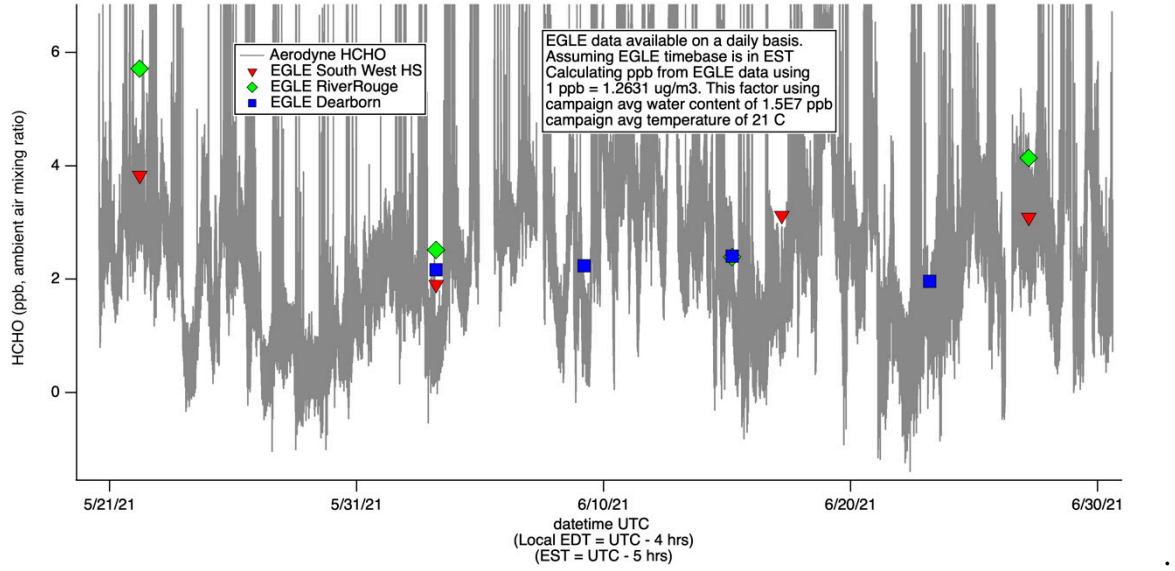

Figure S9. Comparison between AML HCHO data and EGLE monitoring station HCHO data.

NO2 ppb and NO ppb

The TILDAS-FD that measures NO and NO_2 used lasers that were very cold and suffered some data dropouts and issues during portions of the MOOSE campaign due to overheating. This occurred most frequently with NO_2, and the reported data during these dropouts does not show spikes as expected with NOx. On 6/19/2021, the NO_2 laser was switched to a warmer region to reduce such dropouts.

Additionally, the mixing ratios were subject to "motion-sickness" during drives, which can be most easily noticed in the negative deviations in mixing ratios. Occasionally, bad auto backgrounds in motion caused an effective negative offset in reported NO and/or NO_2 for a 15-minute period.

NO was calibrated based on measurements of a NO calibration tank (Supertank 4). NO_2 calibrations were also done throughout the campaign, but that tank (FIREX-CO_2) is known to be low. For this reason, the NOx instrument was used to tie the NO_2 calibration to be tied to the NO tank. This is summarized in the table below.

Table S5. Calibration factor summary for NO, NO_2 and NOx.

		NOx	**NO**	**NO_2**	**NO_2 old line after 6/19 18:59**
Supertank 4 (ST4)	Avg	1.114	0.865	-	-
	Std Dev	0.127	0.065	-	-
FIREX CO_2	Avg	0.555	-	0.428	0.412
	Std Dev	0.065	-	0.013	-
10.1 ppm Tank	Avg	0.8255	-	0.667	-
	Std Dev	-	-	-	-
		Corrected FIREX CO_2 vs ST4		NO_2 cal factor, transferring FIREX CO_2 from ST4	
		0.498		0.860	0.827

The sum of NO and NO_2 is compared to the measured NOx from the CAPS-NOx instrument. The sum agrees well, but is high by 3%, as shown below.

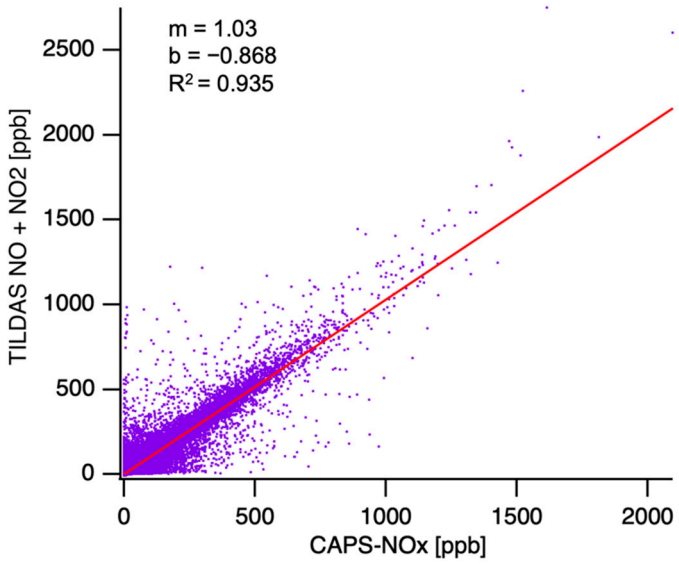

Figure S10. Comparison of TILDAS NOx (NO + NO_2) with CAPS NOx.

NOx ppb

NOx was measured by reaction with ozone and detection by NO_2 using the CAPS-NOx instrument. A Nafion dryer is used prior to the instrument, and as such this is a dry air mixing ratio. Starting around 6/28/21 15:48:22 UTC, reported NOx was lower than expected, and agreed instead with measured NO_2. This indicates a failure in the ozonator that is used to transform NO into NO_2 for detection via CAPS. This data has been excised. Instead, the sum of NO and NO_2, divided by 1.03 as in Figure S10 above, was used for this period.

SO_2 ppb

This data was collected on a Teledyne T100 SO_2 analyzer, which is a UV fluorescence instrument. The SO_2 is a 1-minute measurement. It was interpolated onto the 1-second

time base. This instrument sampled from the main gas phase inlet (at a similar spot to the CO_2 measurement, e.g.). It would have experienced zero-gas additions every 15 minutes for 30 seconds, but the timescale of these zeroes is insufficient to appear in the data. No zero correction has been applied. This instrument's clock was offset. The raw data timestamp required an offset of +14041.2 seconds to yield UTC time. This time offset was determined based on power outage data gaps, and correlations with CO_2.

S2.1.6 Masks

mask_noTraffic

This mask attempts to filter out data that is affected by spikes of CO or NOx from nearby traffic or self-sampling.

1: good data unaffected by traffic or self-sampling.

0: data possibly affected by traffic or self-sampling.

This mask uses as its base data equal to the sum of CO and 10 xNOx. The factor of 10 for NOx aims to balance the fact that gasoline vehicles emit much higher CO concentrations than diesel vehicles do NOx. A 2-minute minimum for this combined trace is calculated, and data exceeding 100 above that difference is deemed "traffic" and the mask set to 0 (so >100 ppb CO or >10 ppb NOx, or a combination). Data within the threshold is deemed "noTraffic" and the mask is set to 1. Periods of self-sampling manually noted during the campaign are set to 0.

A similar strategy can be used to calculate an ozone background trace unaffected (or less affected) by on-road NOx titration.

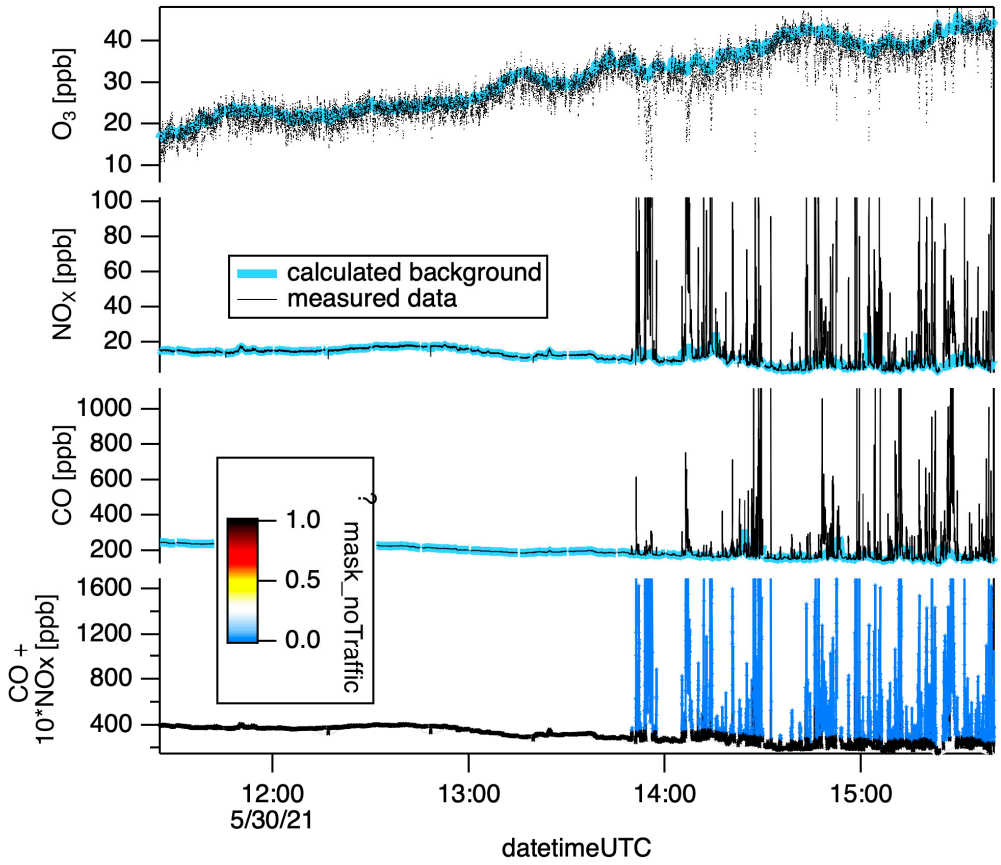

Figure S11. Data with and without traffic mask.

```
// 5 min minimum
```

```
Setdatafolder root:unifiedData; duplicate/o CO_ppb sum_CONOx
sum_CONOx = CO_ppb + 10*NOx_ppb
//sum_CONOx = numtype(NOx_ppb)==2 ? CO_ppb[p] : sum_CONOx[p]
//sum_CONOx = numtype(CO_ppb)==2 ? 10*NOx_ppb[p] : sum_CONOx[p]

QAQCw_fiveminMinimum(datetimeUTC,sum_CONOx,resolution=120)

duplicate/o sum_CONOx_5minMin delta
delta = sum_CONOx - sum_CONOx_5minMin

duplicate/o sum_CONOx, mask_NoTraffic
mask_noTraffic = 1
mask_noTraffic = delta[p] > 100 ? 0 : 1

duplicate/o CO_ppb bg_CO_ppb; bg_CO_ppb = Mask_notraffic[p] ? bg_co_ppb[p] : nan
duplicate/o NOx_ppb bg_NOx_ppb; bg_NOx_ppb = Mask_notraffic[p] ? bg_NOx_ppb[p] : nan
duplicate/o HCHO_ppb bg_HCHO_ppb; bg_HCHO_ppb = Mask_notraffic[p] ? bg_HCHO_ppb[p] : nan
QAQCw_interpOverNaNs_Irrev(datetimeUTC, bg_co_ppb)
QAQCw_interpOverNaNs_Irrev(datetimeUTC, bg_NOx_ppb)
Smooth 120, bg_CO_ppb
Smooth 120, bg_NOx_ppb
bg_CO_ppb = numtype(co_ppb[p])==2 ? NaN : bg_CO_ppb[p]
bg_NOx_ppb = numtype(NOx_ppb[p])==2 ? NaN : bg_NOx_ppb[p]


// Self sampling

setdatafolder root:unifiedData;
duplicate/o CO_ppb mask_selfSampling, mask_class
mask_selfSampling=0; mask_class=0
cast_maskMaker(root:unifiedData:datetimeUTC,root:unifiedData:mask_class,  root:QAQC:QAQC_Start-
Time, root:QAQC:QAQC_EndTime, root:QAQC:QAQC_class)
cast_maskMaker(root:unifiedData:datetimeUTC,root:unifiedData:mask_selfSampling,
root:QAQC:QAQC_StartTime, root:QAQC:QAQC_EndTime, root:QAQC:QAQC_class,whichBit=3)

mask_noTraffic = mask_selfSampling[p] == 1 ? 0 : mask_noTraffic // add self sampling to noTraffic
duplicate/o mask_noTraffic = mask_Traffic; mask_traffic = mask_notraffic[p]==1 ? 0 : 1

// Ozone, unaffected by traffic

duplicate/o O3_ppb neg_O3_ppb
neg_o3_ppb = 120-O3_ppb
QAQCw_fiveMinMinimum(datetimeUTC,neg_o3_ppb,resolution=120)
duplicate/o O3_ppb, deltao3
deltao3 = neg_O3_ppb - neg_o3_ppb_5minmin
duplicate/o deltao3, mask_goodO3; mask_goodO3=1
mask_goodO3 = deltao3[p] > 6 ? 0: 1
duplicate/o O3_ppb bg_O3_ppb; bg_O3_ppb = Mask_goodO3[p] ? bg_O3_ppb[p] : nan
QAQCw_interpOverNaNs_Irrev(datetimeUTC, bg_o3_ppb)
Smooth 120, bg_O3_ppb
bg_o3_ppb = numtype(o3_ppb[p])==2 ? NaN : bg_o3_ppb[p]
```

mask_selfSampling

Self-sampling refers to times when the mobile laboratory sampled its own diesel exhaust, and are characterized by high NOx (particularly NO), N_2O and many other tracers. CO is not a good indicator for diesel exhaust.

Periods of data manually marked as "self" during the field campaign are set to 1. All other times set to 0. These self sampling periods are also counted as traffic in the mask_noTraffic wave described above. This mask is not exhaustive. See Mask_noTraffic for a more comprehensive indicator of exhaust-free air.

Note that manually marked self-sampling periods have been set to NaN (-9999) in the data.

mask_class

The classification of data according to plume types is output as a bitwise mask.

Periods of different classes are allowed to overlap, yielding values that combine those listed in the table below. Use bitwise algebra to extract only a single class of data. An example is shown below the table.

The text notes associated with each of the defined periods is also output in a text file called MOOSE_plumeNotes.txt. These plume descriptions reflect the observations of the operator in the field and have not been vetted.

Table S6. Bitwise variables for defined classes.

Bit	Class Name	Value (2^bit)	Description
0	Good	1	General category for a period of interest
1	NatGas	2	Natural Gas emissions marked by ethane and methane
2	Regional	4	Data during a large regional transect or while stationary doing ozone photochemistry
3	self	8	self sampling. Data contaminated by mobile lab exhaust
4	traffic	16	Data affected by traffic emissions, as evidenced by enhancements of CO and Nox
5	needQA	32	Raw field data requires quality assurance during this time period
6	calibration	64	A calibration was done on one of the gas phase instruments
7	blacklist	128	All data during this time is invalid (e.g. power outage)
8	loop	256	Data collected during a loop around a pre-set path (e.g. Dearborn cloverleaf loop)

An example of bitwise algebra is shown below. This Igor Pro code uses mask_class to create a new mask_regional.

```
Duplicate/o mask_class, mask_regional
Mask_regional = 0
Mask_regional = mask_class & 2^2  // test bit 2, for regional. This will yield a wave with values of 0 or 4
Mask_regional = mask_regional == 0 ? 0 : 1 // this is now a simple 0 or 1 mask
```

S2.1.7 README for MOOSE_Plumenotes.txt

MOOSE_plumeNotes are live operator notes taken by the Aerodyne Mobile Laboratory scientists during measurements. They are associated with a specific time interval termed a "plume"

These notes have not been edited or vetted.

Any association of a plume with a facility is speculative and subject to revision by Aerodyne scientists. Facility names may not be accurate.

No use or publication of these notes is permitted without explicit consent of Tara Yacovitch (Aerodyne Research, Inc.) and Jay Olaguer (Michigan EGLE).

S2.2. Vocus PTR TOF-MS

Please direct all questions relating to this dataset to: Manjula Canagaratna, mrcana@aerodyne.com

Last updated – May 25, 2022 – ICARTT File Revision R2

The Vocus Proton Transfer Reactor Time of Flight Mass Spectrometer (Vocus PTR-TOFMS) was deployed on the Aerodyne Mobile Laboratory (AML). This instrument measured the time of flight of several gas-phase volatile organic compounds (VOCs), converting them to mass-to-charge ratios using mass calibration parameters. Each of the signals was detected as voltages and converted to ions per second. It sampled through a ¼" Teflon tube with a particle filter on the exterior tip.

Data

The table below lists the compounds that were output to the VocusPTRMS-VOC DataID . The raw data collected was processed using custom software based on Igor Pro (Tofware, by TOFWERK and Aerodyne Research Inc). The updated data output includes high-resolution ions reported in parts-per-billion (ppb) concentrations (highlighted cells below). The concentrations (in ppb) of high-resolution ions as a function of time are identified by their wave names. Calibrations and zeros were performed for these species, allowing for corrections for instrument background and instrument sensitivity as a function of sampling time.

A 3s inlet lag was also utilized, which approximately aligns the Vocus traces to the CO and CO_2 signals from the gas phase tracers (see DataID: AMLGAS, PI: Yacovitch). When data from 2 different instruments is to be compared or correlated, it will still be necessary to optimize and correct for these small errors in time in order to get the most accurate tracer ratios.

The table below lists all waves reported, and the best fit calibration factor obtained by fitting the observed data in counts-per-second with the calibrated concentrations estimated in counts-per-ppb. Three distinct time periods with calibration factors that vary on the order of 30% were observed for all ions. Within each time period the variation in calibration factor for ions was generally <15%. Note that the variations in the calibration factor as a function of time were accounted for in the analysis.

For species that were not calibrated, the measured ion counts per second (cps) were converted to ppb using the previously published method of Sekimoto et al. [7] from estimated molecular properties. For each species that was calibrated, the variation in sensitivity (cps/ppb) with known proton capture rate constant was plotted. The sensitivity (cps/ppb) vs. capture rate constant plot for the calibrated species was then plotted and the fitted slope was utilized to estimate sensitivities for the uncalibrated species whose capture rate constants were estimated according to Sekimoto et al. [7]. The fitted slope varied across two broad time periods. For the time period between 5/21 and 6/20 15:21 the distribution of slopes was 816 +/ 20% (1 sigma). After 6/20 15:21, the slopes of this plot increased to 1041 +/- 20% (1 sigma). These two slopes were utilized to calculate the concentrations of the uncalibrated species in ppb during the different time periods.

The high-resolution ion formulas listed in the table could correspond to several potential species of interest. It is important to note that there may be other species or isomers not listed at that mass that may contribute to signal enhancements. Fragments or clusters of the analyte with water or other high-concentration species may also contribute to the signal. As shown in in Pagonis et al. [8], even ions that have only one species listed under potential assignments can have contributions from fragmentation of larger parent species. Thus, caution must be exercised when interpreting the identities of all observed Vocus PTR ions. For example, in urban measurements, $C_6H_6H^+$ ions observed in proton transfer spectra is often identified with benzene. However, as shown in Figure S12 below, direct comparisons of the concentrations obtained for C_6H_7+ (assuming benzene sensitivities determined from the calibration tank) during Moose with those obtained from the GC EI-TOF indicate that the C_6H_6H+ likely has multiple contributions in addition to benzene.

There are a few data gaps. A gap on 6/5/2021 (~10 hours) was due to a breaker issue in the mobile lab. A gap on 6/21/2021 (~2 days) was due to a blown fuse on the Vocus;

another on 6/26/2021 (~18 hrs) was due to a power outage at the site due to regional flooding. UMR_129 (includes naphthalene) is reported without further high-resolution analysis. No data is reported for UMR_185, nominally isoflurane. Comparison with GC-EI-ToF isoflurane enhancements showed no activity in the Vocus instrument at these times. No data is reported for C11 aromatics (C11H17).

These data may be subject to future revision and require prior OK from data PI before publication.

Table S7. List of reported ions from Vocus PTR-ToF .

Wave Name	Standard Name	Long description	Ion of Interest	Cal factor (cps/ppb)	Data status
Time_Start	Time_Start	number of seconds since 00:00:00 UTC	-	-	
julianDay	Platform_julianDay_InSitu_None	Julian Day 140 is May 20th, 2021	-	-	
C2H5O_ppb	Gas_acetaldehyde_InSitu_S_AMF	C2H4O, acetaldehyde (and ethylene oxide)	$C_2H_4OH^+$		
CH5S_ppb	Gas_CH3SH_InSitu_S_AMF	CH3SH, methane thiol aka methyl mercaptan	CH_4SH^+		
C3H5O_ppb	Gas_acrolein_InSitu_S_AMF	C3H4O, acrolein	$C_3H_4OH^+$		
C3H7O_ppb	Gas_acetone_InSitu_S_AMF	C3H6O, acetone	$C_3H_6OH^+$	3752	
C4H5O_ppb	Gas_furan_InSitu_S_AMF	C4H4O, furan	$C_4H_4OH^+$		
C5H7_ppb	Gas_cyclopentadiene_InSitu_AMF	C5H6, cyclopentadiene	$C_3H_6OH^+$		
C5H9_ppb	Gas_isoprene_InSitu_S_AMF	C5H8, isoprene	$C_5H_8H^+$	921	
C4H9O_ppb	Gas_ButanalMEK_InSitu_M_AMF	C4H8O, sum of methyl ethyl ketone and butanal	$C_4H_8OH^+$	3029	
C6H7_ppb	Gas_benzene_InSitu_S_AMF	C6H6, benzene	$C_6H_6H^+$	1314	
C4H9O2_ppb	Gas_EthAcetate_InSitu_S_AMF	C4H8O2, ethyl acetate and pyruvic acid	$C_3H_4O_3H^+$, $C_4H_8O_2H^+$		
C7H9_ppb	Gas_toluene_InSitu_S_AMF	C7H8, toluene	$C_7H_8H^+$		

Wave Name	Standard Name	Long description	Ion of Interest	Cal factor (cps/ppb)	Data status
C6H7O_ppb	Gas_Phenol_InSitu_S_AMF	C6H5OH, phenol	$C_6H_6OH^+$		
C8H11_ppb	Gas_C8aromatics_InSitu_M_AMF	C8H10, sum of C8 aromatics (m- o- and p-xylene and ethylbenzene)	$C_8H_{10}H^+$	3900	
C9H13_ppb	Gas_C9aromatics_InSitu_M_AMF	C9H12, sum of C9 aromatics (includes trimethylbenzene, etc.)	$C_9H_{12}H^+$	4094	
UMR_129	Gas_Naphthalene_InSitu_S_AMF	C10H8, naphthalene, measured at m/z 129	$C_{10}H_8H^+$		
C10H17_ppb	Gas_Monoterpenes_InSitu_M_AMF	C10H16, sum of monoterpenes (includes alphapinene, limonene, etc.)	$C_{10}H_{16}H^+$	1620	
S6H_Hz	Gas_Hexasulfur_InSitu_S_AMF	S6, hexasulfur, measured at m/z 193 as S6H+	S_6H^+		
UMR_185	Gas_Isoflurane_InSitu_S_AMF	C3H2ClF5O, isoflurane, measured at m/z 185	$C_3H_2ClF_5OH^+$		No data
C10H15_ppb	Gas_C10aromatics_InSitu_M_AMF	C10H14, sum of C10 aromatics	$C_{10}H_{14}H^+$		
C11H17_ppb	Gas_C11aromatics_InSitu_M_AMF	C11H16, sum of C11 aromatics	$C_{11}H_{16}H^+$		No data

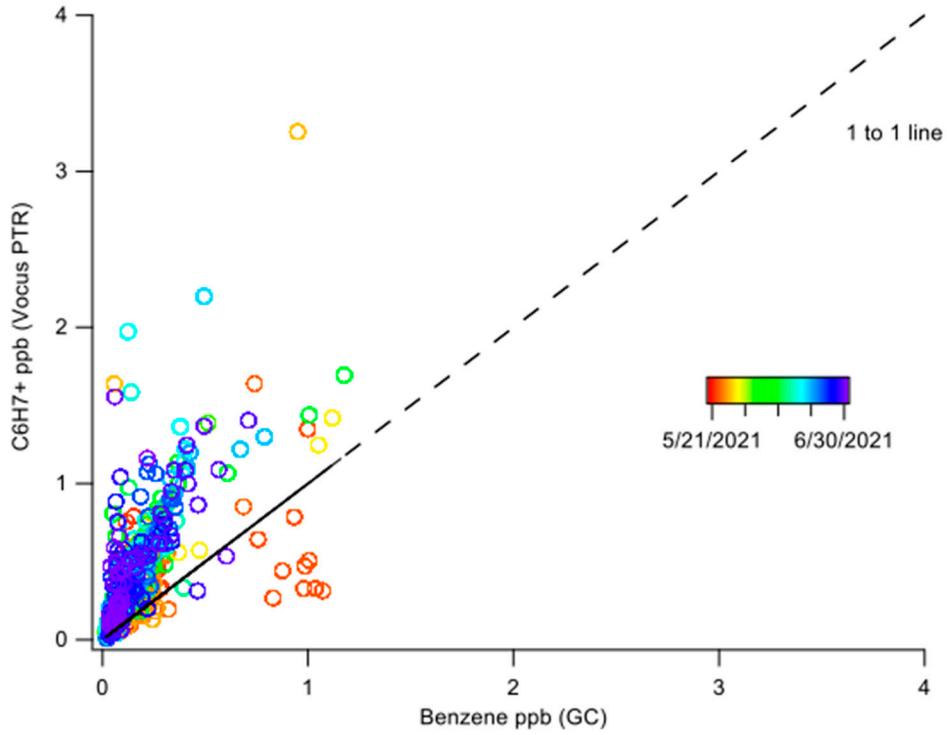

Figure S12. Comparison of Vocus PTR-ToF-MS) C_6H_7+ signal (converted to ppb) with the GC EI-ToF-MS signal obtained for benzene. The plot is colored by time. .

S3. Point Source Chemical Signatures

S3.1. MA130 (Industrial Coatings)

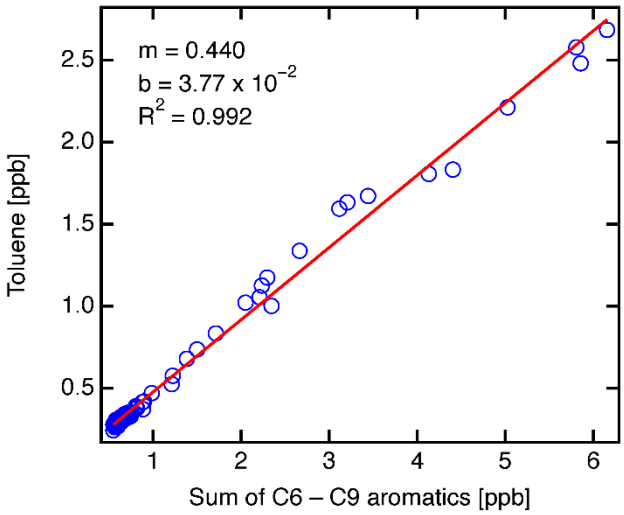

Figure S13. Example correlation plot showing how the ratio of toluene to total aromatics is determined for plume 181 shown the main text, and in the figure below.

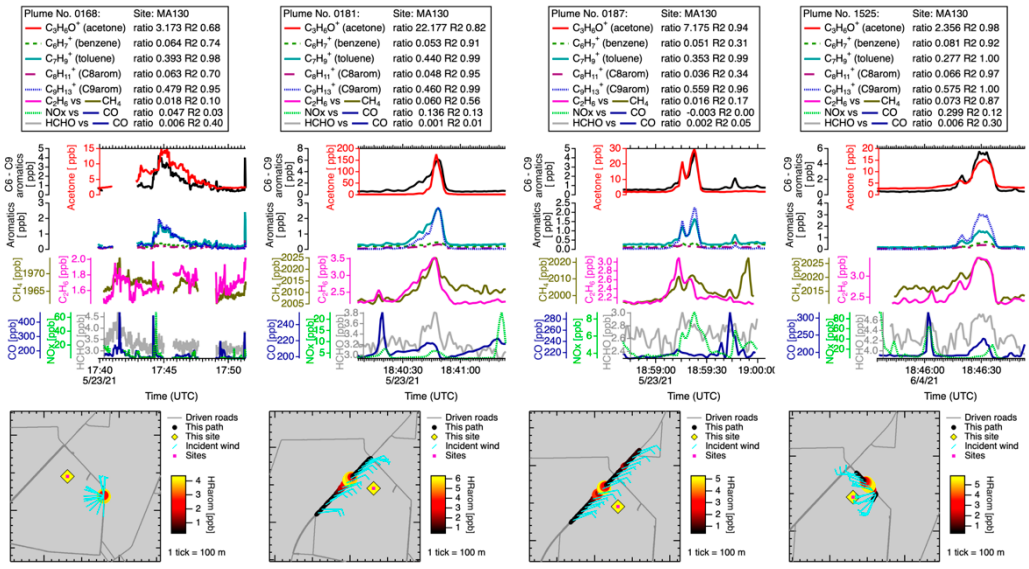

Figure S14. Plumes from site MA130. Ratios of VOCs to the sum of aromatics and R2 of the linear fit are listed beside their trace name (top). Additional ratios for other gas phase tracers are noted versus their denominator. Time traces for selected traces are shown (middle). A map (bottom) shows concentration over the driven path.

S3.2. MA237 (Industrial Cleaning)

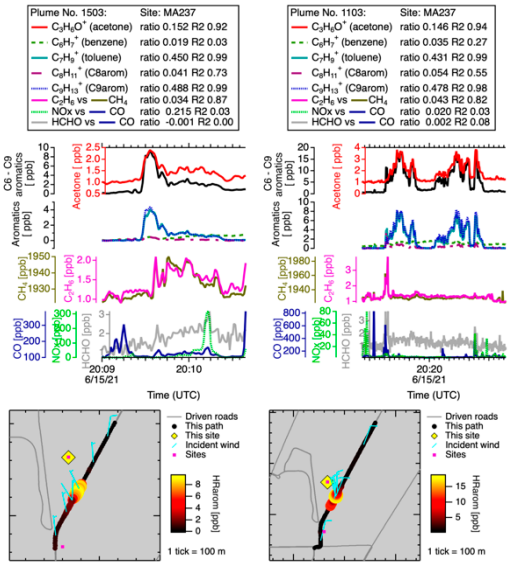

Figure S15. MA237 measurements on 6/15/21.

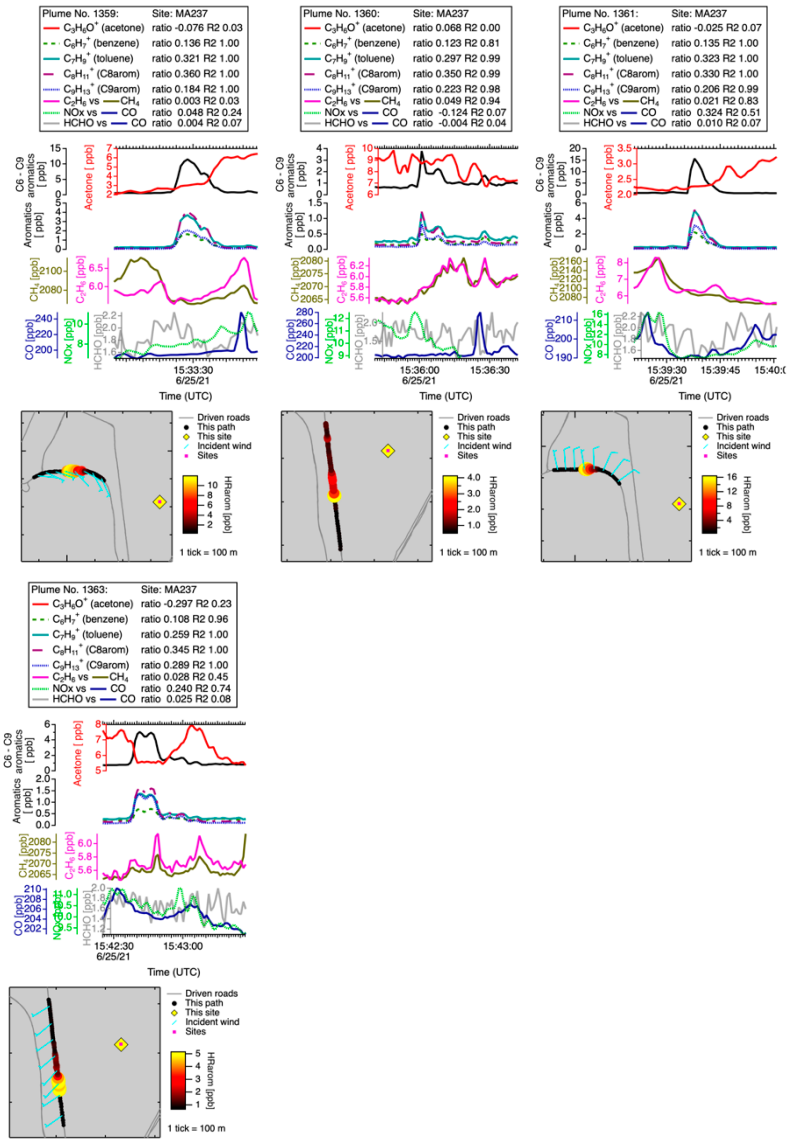

Figure S16. MA237 Measurements on 6/25/21.

S3.3. SA96 (Adhesives manufacturer)

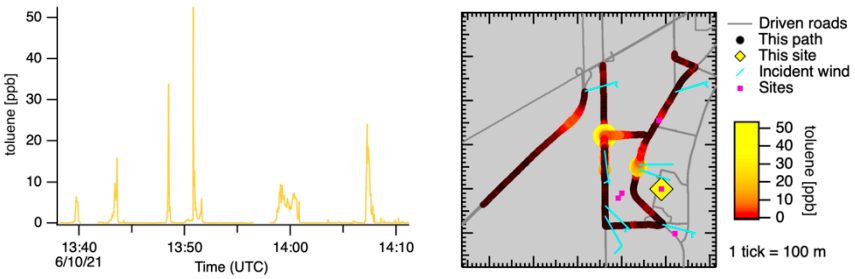

Figure S17. Overview of SA96 measurements on 10-June-2021 (plume 1531), log scale toluene.

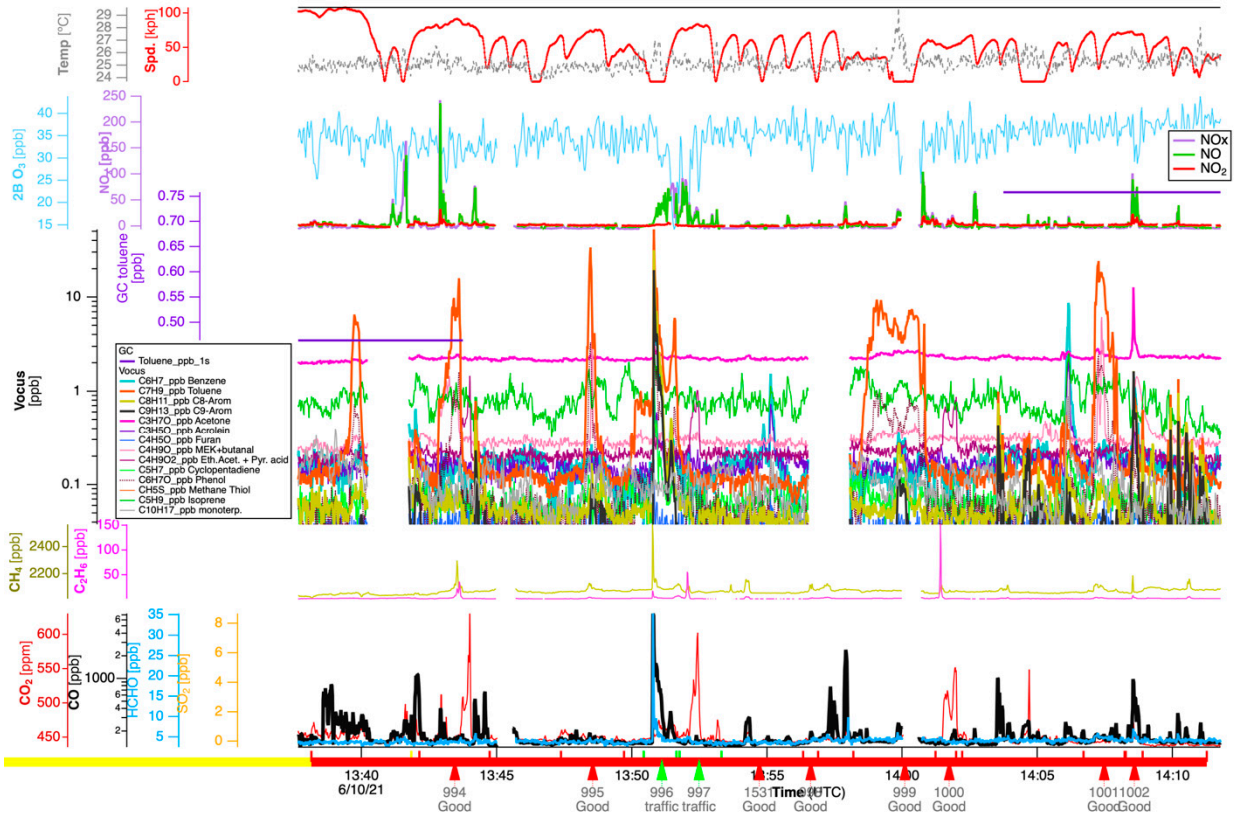

Figure S18. Phenol (dotted line) is also present and correlated with toluene (orange).

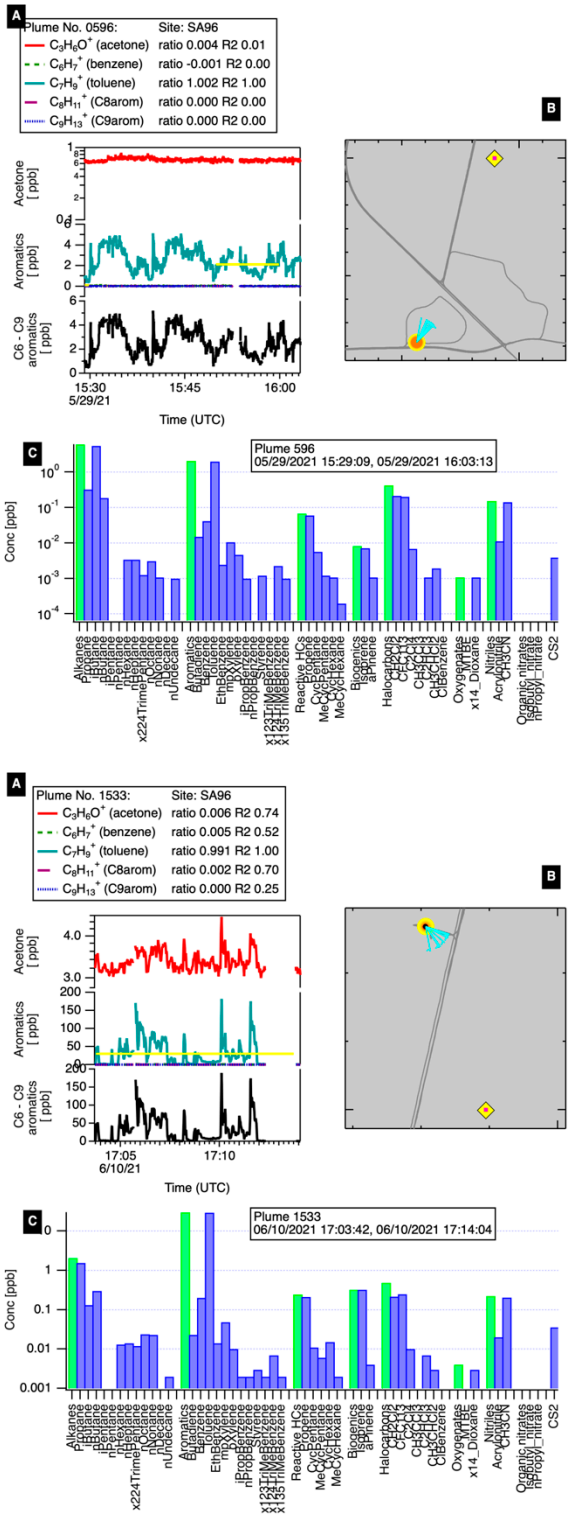

Figure S19. Results of two stationary GC measurements downwind of SA96. Toluene dominates the aromatics. Note the toluene concentration during the GC sample period is indicated by the yellow line in panel A.

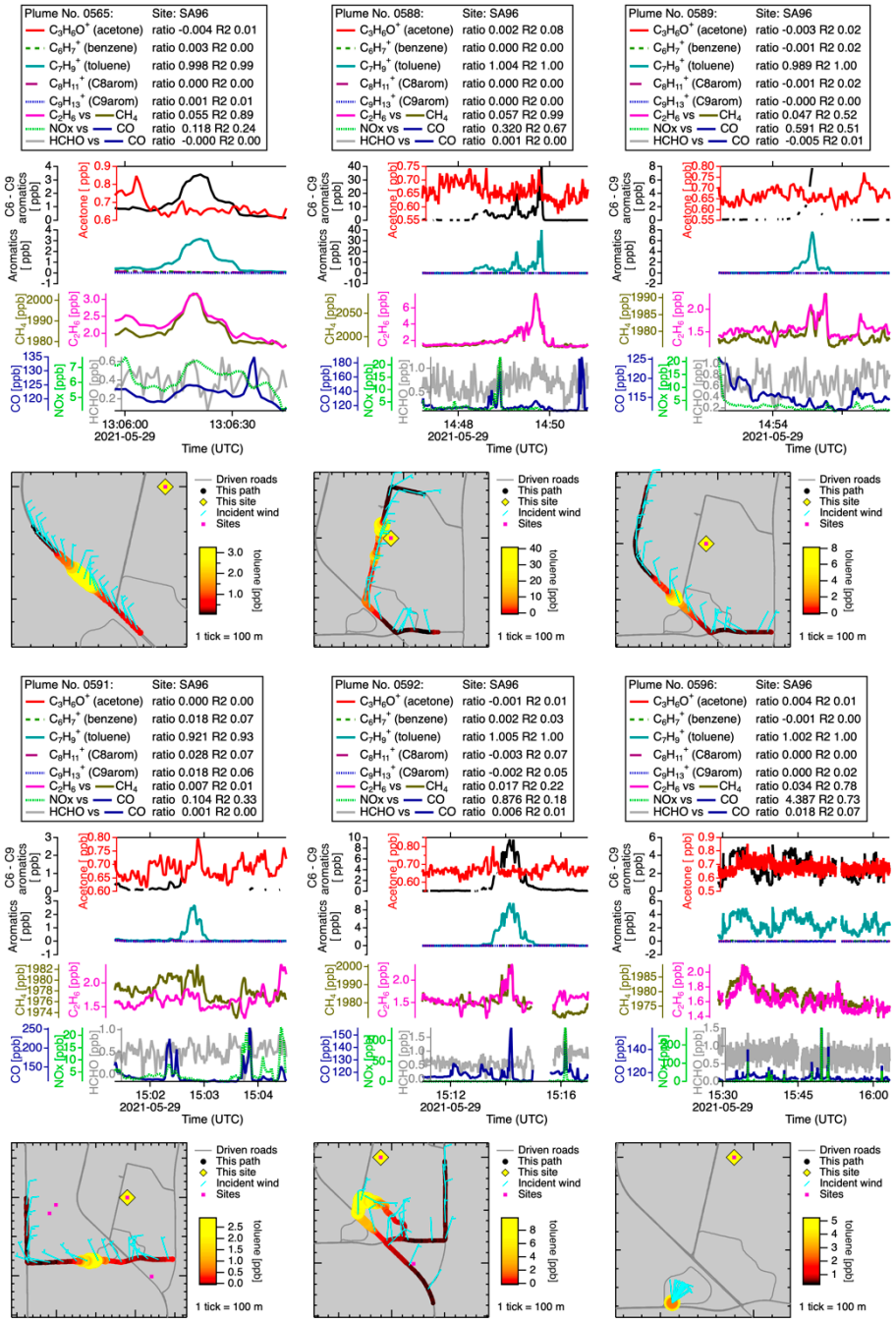
Plume No. 0565: Site: SA96
C3H6O+ (acetone) ratio -0.004 R2 0.01
C6H7+ (benzene) ratio 0.003 R2 0.00
C7H9+ (toluene) ratio 0.998 R2 0.99
C8H11+ (C8arom) ratio 0.000 R2 0.00
C9H13+ (C9arom) ratio 0.001 R2 0.01
C2H6 vs CH4 ratio 0.055 R2 0.89
NOx vs CO ratio 0.118 R2 0.24
HCHO vs CO ratio -0.000 R2 0.00
Plume No. 0588: Site: SA96
C3H6O+ (acetone) ratio 0.002 R2 0.08
C6H7+ (benzene) ratio 0.000 R2 0.00
C7H9+ (toluene) ratio 1.004 R2 1.00
C8H11+ (C8arom) ratio 0.000 R2 0.00
C9H13+ (C9arom) ratio 0.000 R2 0.00
C2H6 vs CH4 ratio 0.057 R2 0.99
NOx vs CO ratio 0.320 R2 0.67
HCHO vs CO ratio 0.001 R2 0.00
Plume No. 0589: Site: SA96
C3H6O+ (acetone) ratio -0.003 R2 0.02
C6H7+ (benzene) ratio -0.001 R2 0.02
C7H9+ (toluene) ratio 0.989 R2 1.00
C8H11+ (C8arom) ratio -0.001 R2 0.02
C9H13+ (C9arom) ratio -0.000 R2 0.00
C2H6 vs CH4 ratio 0.047 R2 0.52
NOx vs CO ratio 0.591 R2 0.51
HCHO vs CO ratio -0.005 R2 0.01
C6 - C9 aromatics [ppb]
Acetone [ppb]
Aromatics [ppb]
CH4 [ppb]
C2H6 [ppb]
CO [ppb]
NOx [ppb]
HCHO [ppb]
13:06:00
13:06:30
2021-05-29
Time (UTC)
14:48
14:50
14:54
Driven roads
This path
This site
Incident wind
Sites
toluene [ppb]
1 tick = 100 m
Plume No. 0591: Site: SA96
C3H6O+ (acetone) ratio 0.000 R2 0.00
C6H7+ (benzene) ratio 0.018 R2 0.07
C7H9+ (toluene) ratio 0.921 R2 0.93
C8H11+ (C8arom) ratio 0.028 R2 0.07
C9H13+ (C9arom) ratio 0.018 R2 0.06
C2H6 vs CH4 ratio 0.007 R2 0.01
NOx vs CO ratio 0.104 R2 0.33
HCHO vs CO ratio 0.001 R2 0.00
Plume No. 0592: Site: SA96
C3H6O+ (acetone) ratio -0.001 R2 0.01
C6H7+ (benzene) ratio 0.002 R2 0.03
C7H9+ (toluene) ratio 1.005 R2 1.00
C8H11+ (C8arom) ratio -0.003 R2 0.07
C9H13+ (C9arom) ratio -0.002 R2 0.05
C2H6 vs CH4 ratio 0.017 R2 0.22
NOx vs CO ratio 0.876 R2 0.18
HCHO vs CO ratio 0.006 R2 0.01
Plume No. 0596: Site: SA96
C3H6O+ (acetone) ratio 0.004 R2 0.01
C6H7+ (benzene) ratio -0.001 R2 0.00
C7H9+ (toluene) ratio 1.002 R2 1.00
C8H11+ (C8arom) ratio 0.000 R2 0.00
C9H13+ (C9arom) ratio 0.000 R2 0.02
C2H6 vs CH4 ratio 0.034 R2 0.78
NOx vs CO ratio 4.387 R2 0.73
HCHO vs CO ratio 0.018 R2 0.07
15:02
15:03
15:04
15:12
15:16
15:30
15:45
16:00

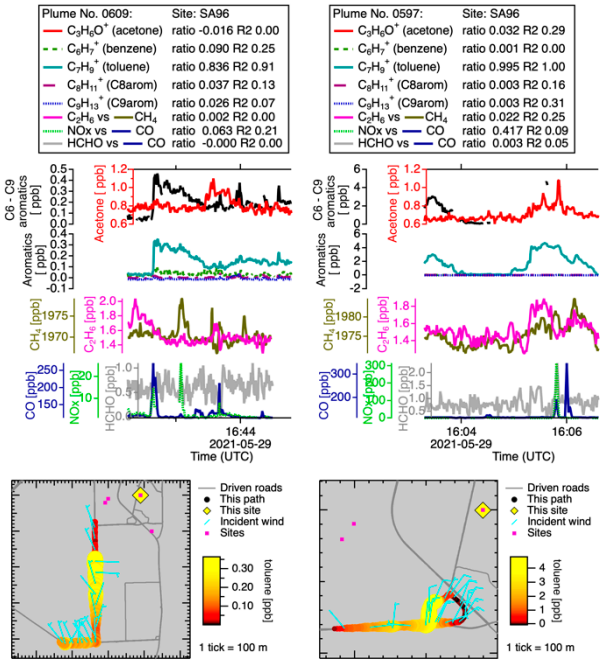

Figure S20. Plumes at SA96 on 29-May-2021.

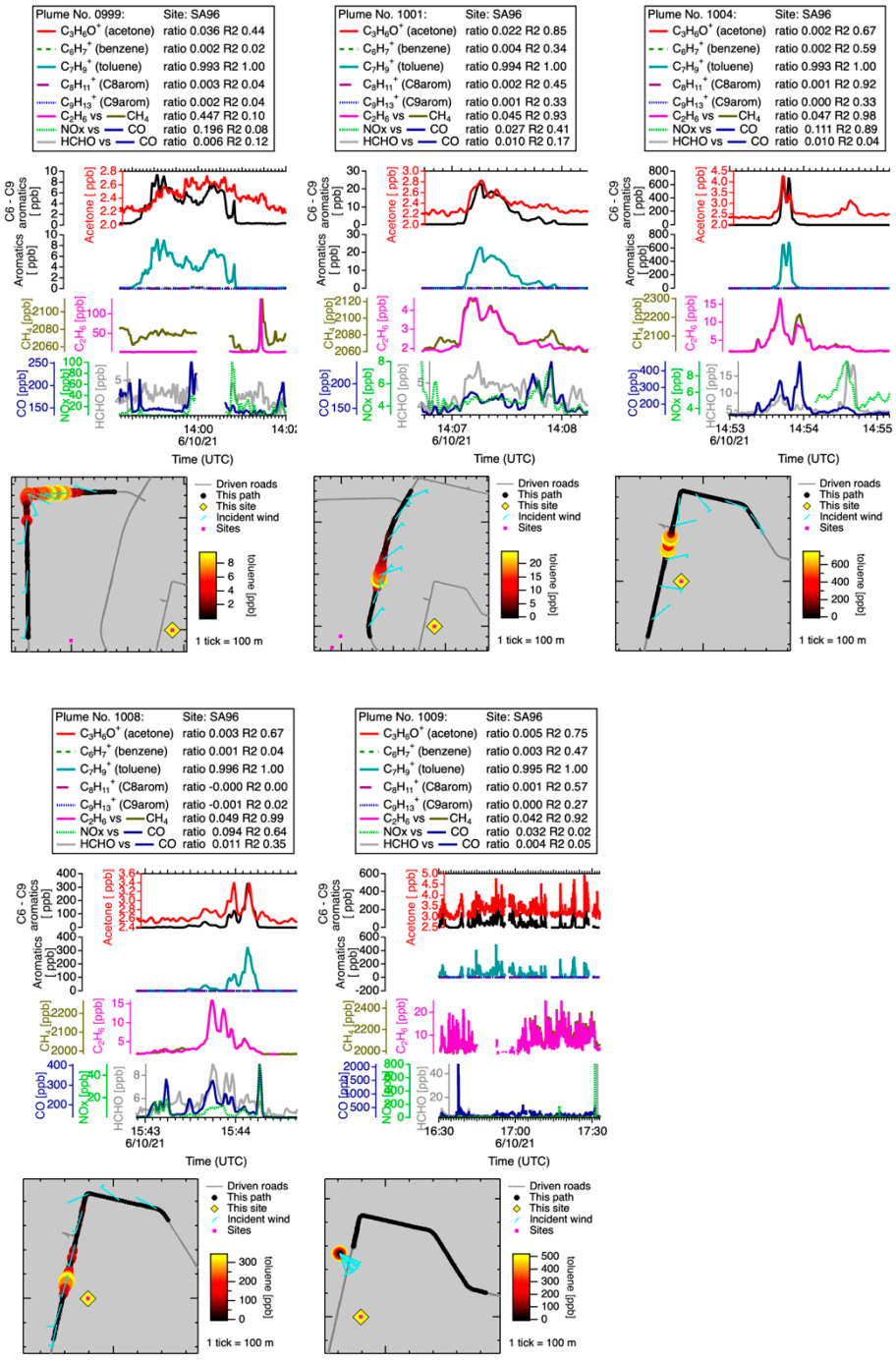

Figure S21. Plumes at SA96 on 10-June-2021.

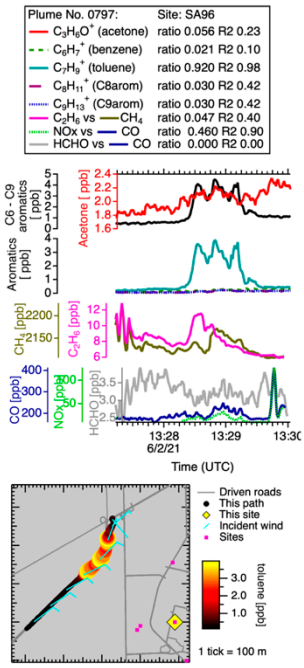

Figure S22. Plume at SA96 on another day.

S3.3. WA236 (Chemical Waste), and nearby sources

Site WA236 is a chemical waste company with on-site storage. This facility is in an area near numerous other sources including WA248, a facility treating waste oils and wastewater and two automaker facilities: WA137, an assembly plant, and WA27, an engine plant. Two additional unknown sources were present. The first is a mixed VOC source observed NE of the WA27 engine plant. The second is some source to the west or SW of the WA236 chemical waste facility, that emitted methane thiol, but no BTEX or acetone (possibly a biogenic source). Finally on the map below, a rail yard and test track are called out, but these areas did not show significant emissions.

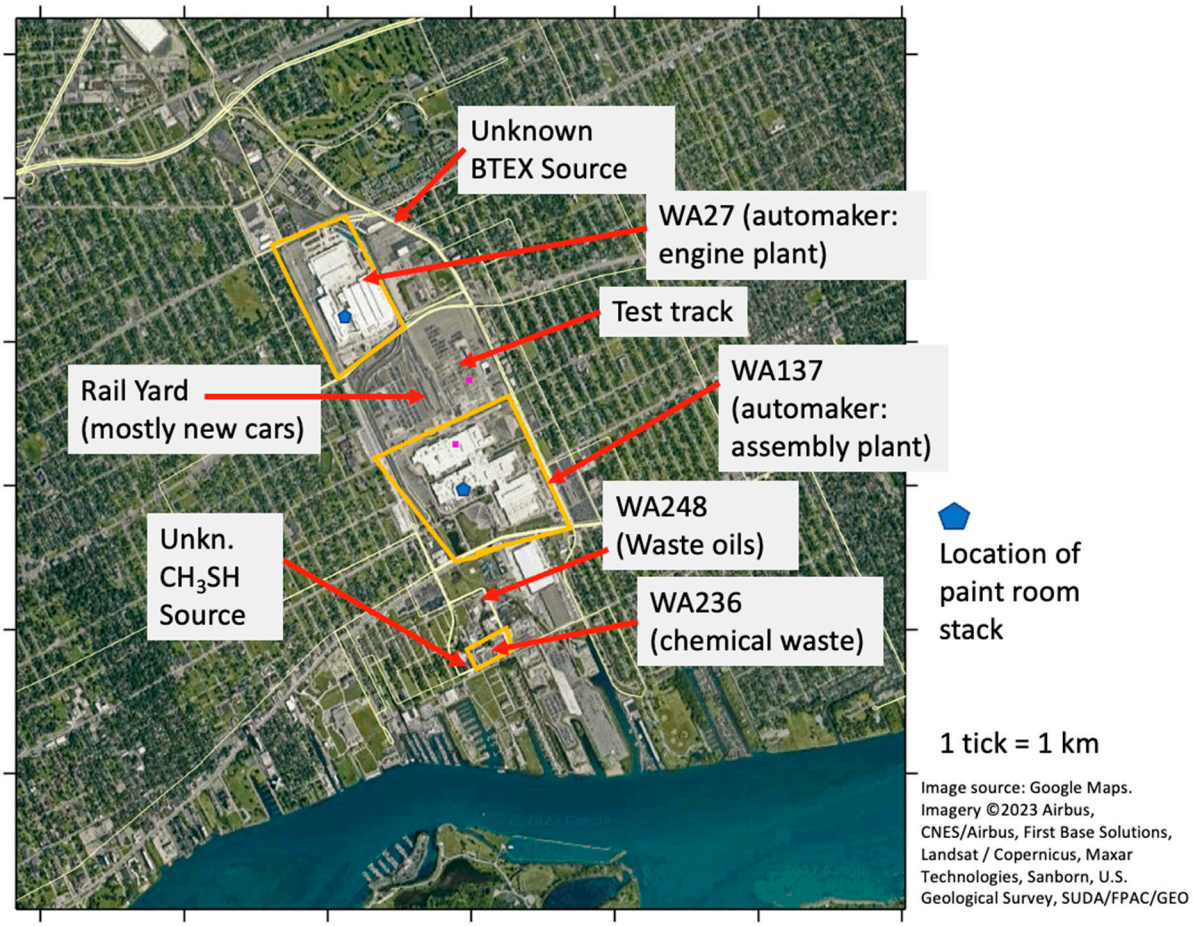

Figure S23. Overview of potential point sources including WA137, an assembly plant, and WA27, an engine plant. WA236, a chemical waste company with on-site storage and WA248, a facility treating waste oils and wastewater. AML-driven paths are shown in pale yellow. Facility borders highlighted in orange.

Various portions of the area above were visited during MOOSE campaign. The automakers WA137 and WA27 were visited on 26-May-2021 (SW winds), 3-June-2021 (SW winds) and 25-June-2021 (SE winds). These visits also captured emissions from WA236, the chemical waste site. WA236 was visited on 27-June-2021 (S wind). No visits to this area occurred in East winds.

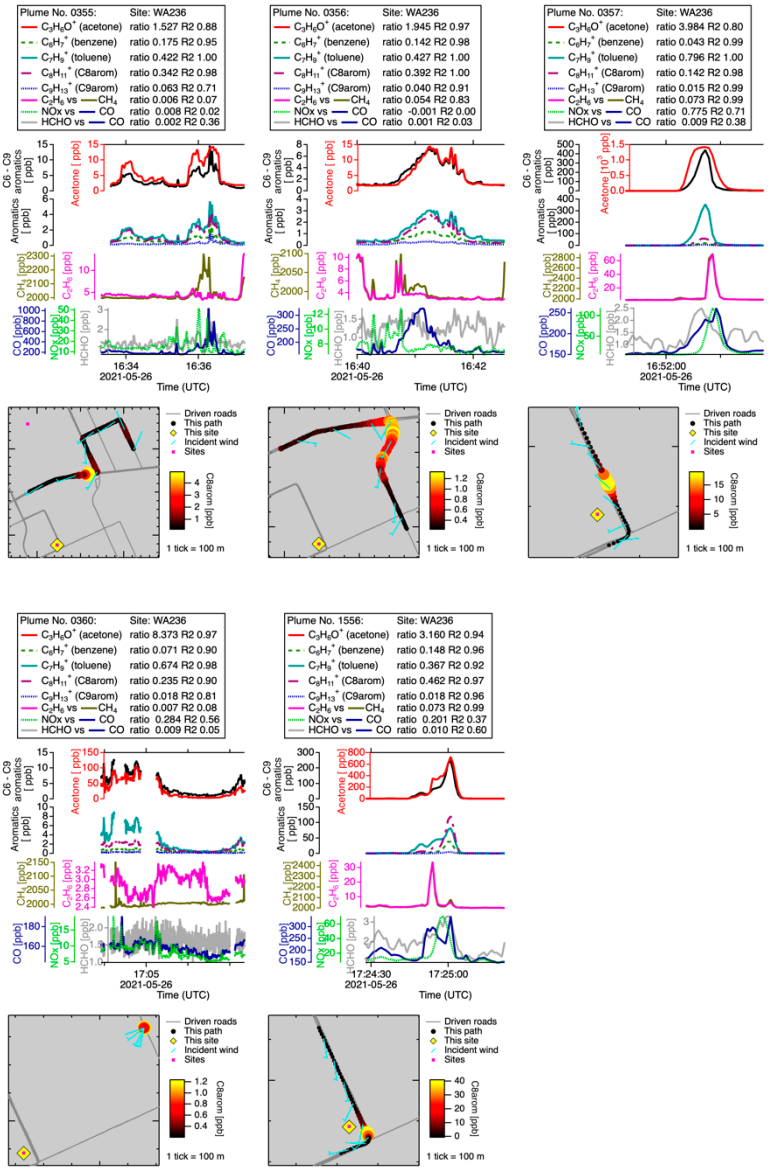

Figure S24. Transects downwind of site WA236 on 26-May-2021.

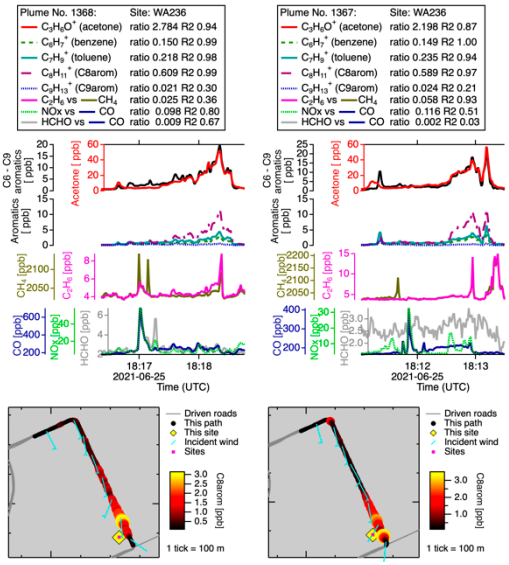

Figure S25. Transects downwind of site WA236 on 25-June-2021.

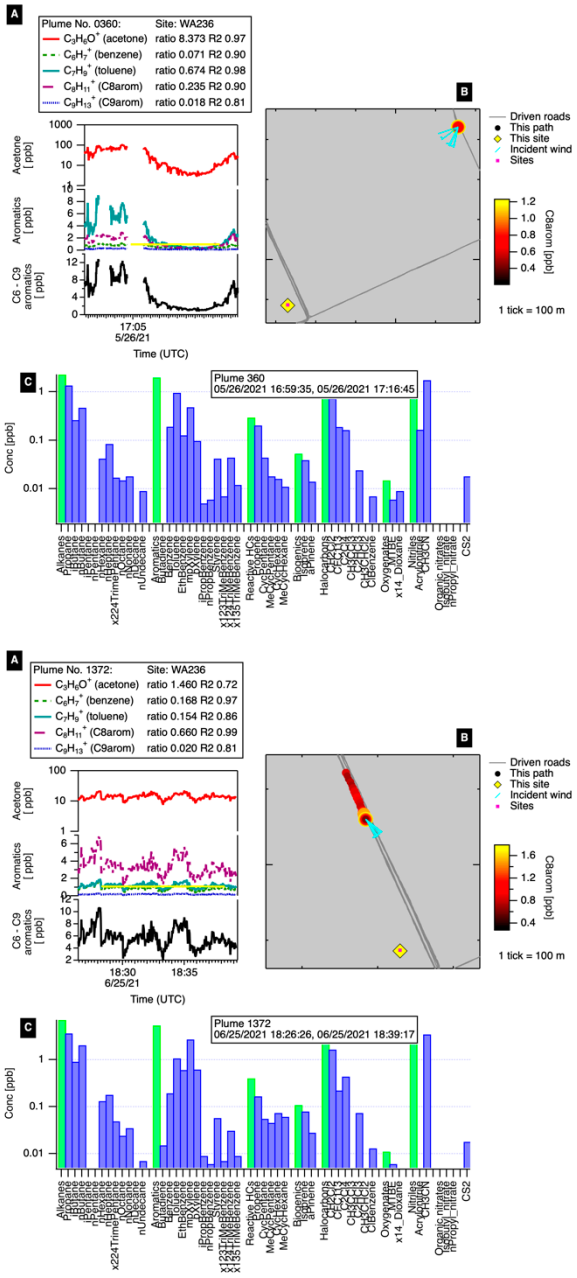

Figure S26. Stationary GC samples of the WA236 plume.

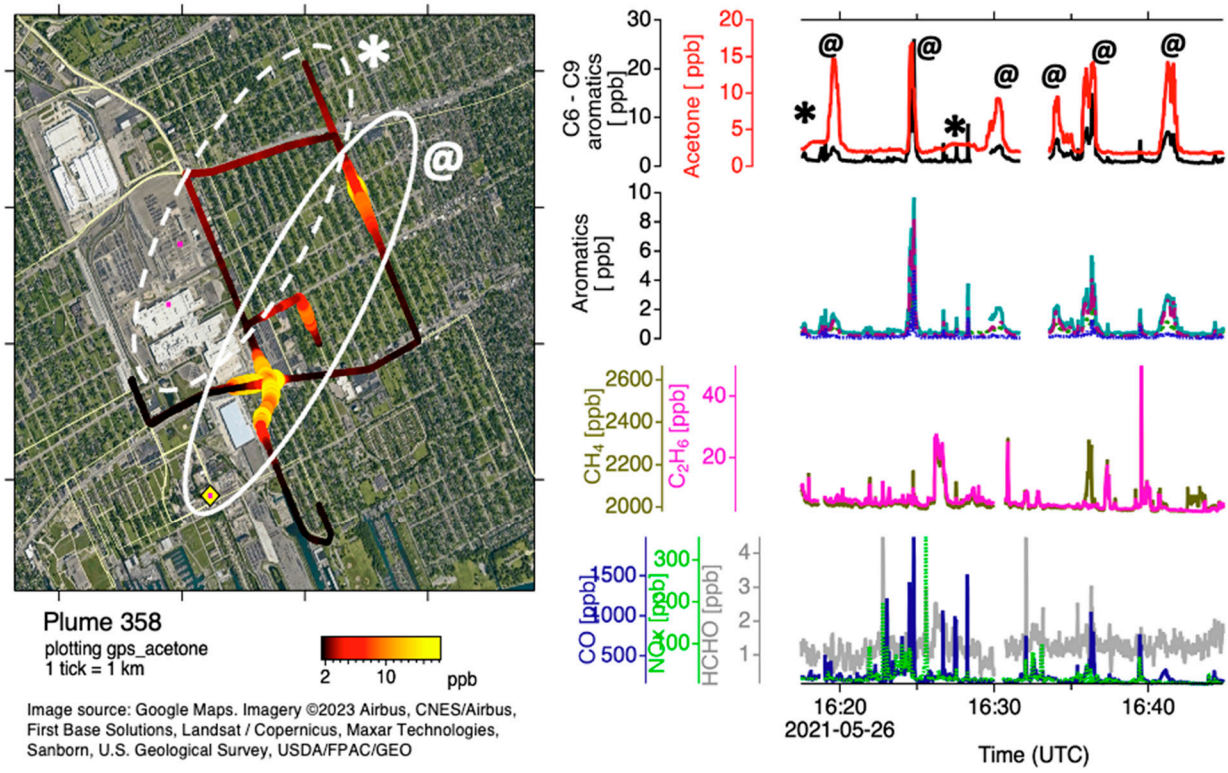

Figure S27. Representative transects downwind of the chemical waste facility WA236 and the automaker assembly plant WA137. The map (left) shows the AML path colored by acetone concentration. The time traces (left) show a primary VOC plume (@ symbol), along with a lower intensity and broader plume (* symbol). These plumes correspond to the circled and labeled areas on the map.

As part of this work we investigated whether the Vocus PTR spectra contained potential fingerprints that were specific to source impacts. Positive matrix factorization, was utilized for this purpose. PMF is a multivariate factor analysis technique developed by Paatero et al. [9,10] to solve the bilinear factor model $x_{ij} = \Sigma_p g_{ip} f_{pj} + e_{ij}$ where x_{ij} are the measured values of j species in i samples, P are factors comprised of constant source profiles (f_j, mass spectral data) with varying contributions over the time period of the dataset (g_i, time series), without any a priori assumptions of either mass spectral or time profile [11,12].

The PMF analysis yields factors which correspond to groups of ions that have similar time trends. The factor mass spectra provide the identities of the grouped ions that and the factor time trends provide the contributions of each group to the measured signal at any given measurement time. In this work 4 distinct factors were identified as shown in Figure S28 and Figure S29.

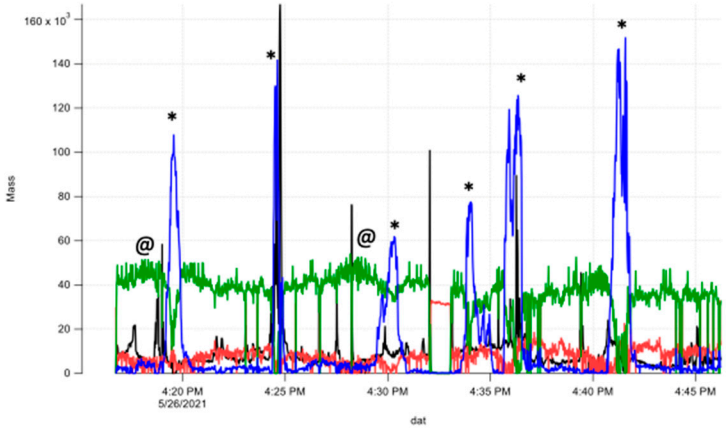

Figure S28. Time series for the 4-factor PMF solution associated with the measurements shown in Figure S27.

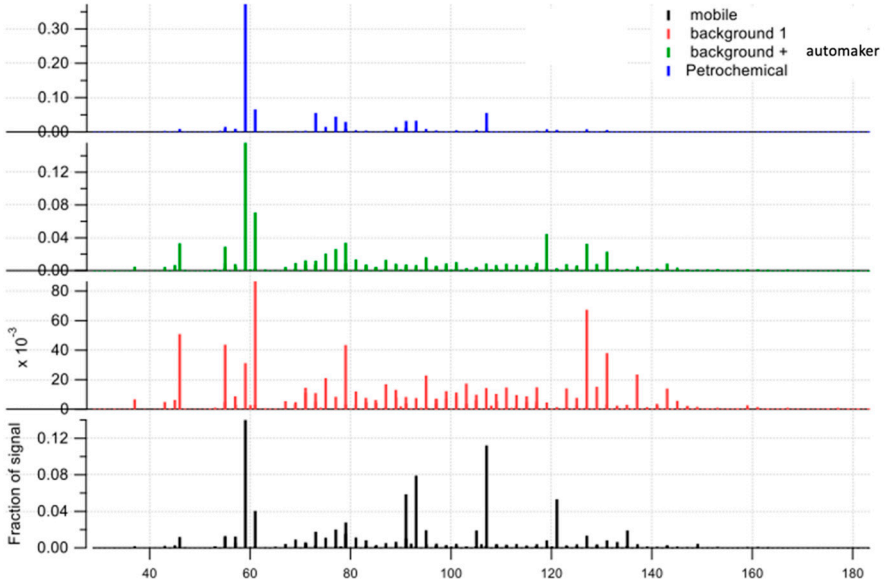

Figure S29. High-resolution mass spectra for the 4-factor PMF solution shown in Figure S28.

Based on the time trends of the factors, chemical composition of mass spectra, and known GPS locations, the factors are identified according to their likely sources. The "petrochemical" factor (blue factor, peaks indicated by * symbol) and mobile sources (aka traffic, black factor) are the most clearly extracted factors. The petrochemical factor is attributed to the plume from WA236. Based on GPS locations and plume intercepts, it is likely that the green factor is impacted by background air as well as possibly by the broad automaker assembly plant WA137 plume (@ symbol), which on this day contained primarily acetone. Interestingly, a key ion for this factor was at m/z 119.035, with potential chemical assignment of butanedioic acid. Comparisons of the PMF factor mass spectra are used to identify key ion signature of the various factors as shown in Table S8.

Table S8. High-resolution mass-to-charge ratios (m/z) and possible chemical assignments for the key ion(s) present in selected PMF factors.

Petrochemical factor: WA236		**Background + automaker?**		**Mobile**	
59.049	**propanal, acetone**	**59.049**	propanal, acetone	91.054	Aromatic fragment

73.065	butanal, 2-methylpropanal, tetrahydrofuran, 2-butanone	119.035	butanedioc acid	93.07	Toluene and other aromatics
77.06	acetone water cluster, c3 hydroperoxide, propane diols			107.086	C8 aromatics
91.075	butane diols, c4-c4 carbonyl water cluster, ethylene glycol dimethyl ether			121.101	C9 aromatics

Another instance of these plumes propagating through residential neighborhoods is observed on 25-June-2021, as shown in Figure S30. Unfortunately, the wind direction (due south) was such that it was not possible to separate contributions from the 4 potential sources. However, we observe clear differences in the measured plume signatures throughout the plume. Initially, close to the chemical waste site WA236 and neighboring WA248 waste oils facility, the plume contains significant acetone. Further downwind, when the automaker WA137 is included, there proportionately more aromatics. This is demonstrated by comparing the log-scale maps in Figure S30.A (C9-aromatics) and Figure S30.D (Acetone). It can also be seen in the bifurcation of the correlation plot of acetone to total aromatics (Figure S30.B). The observation of aromatics from the WA137 automaker on this day is notable given the observation of an acetone-only plume on 25-May-2021. Whether or not the WA27 engine plant is contributing to the overall emissions cannot be definitively determined in this data. Close-in transects to both waste facilities WA236 and WA248 confirm that both these sites were emitting on this day.

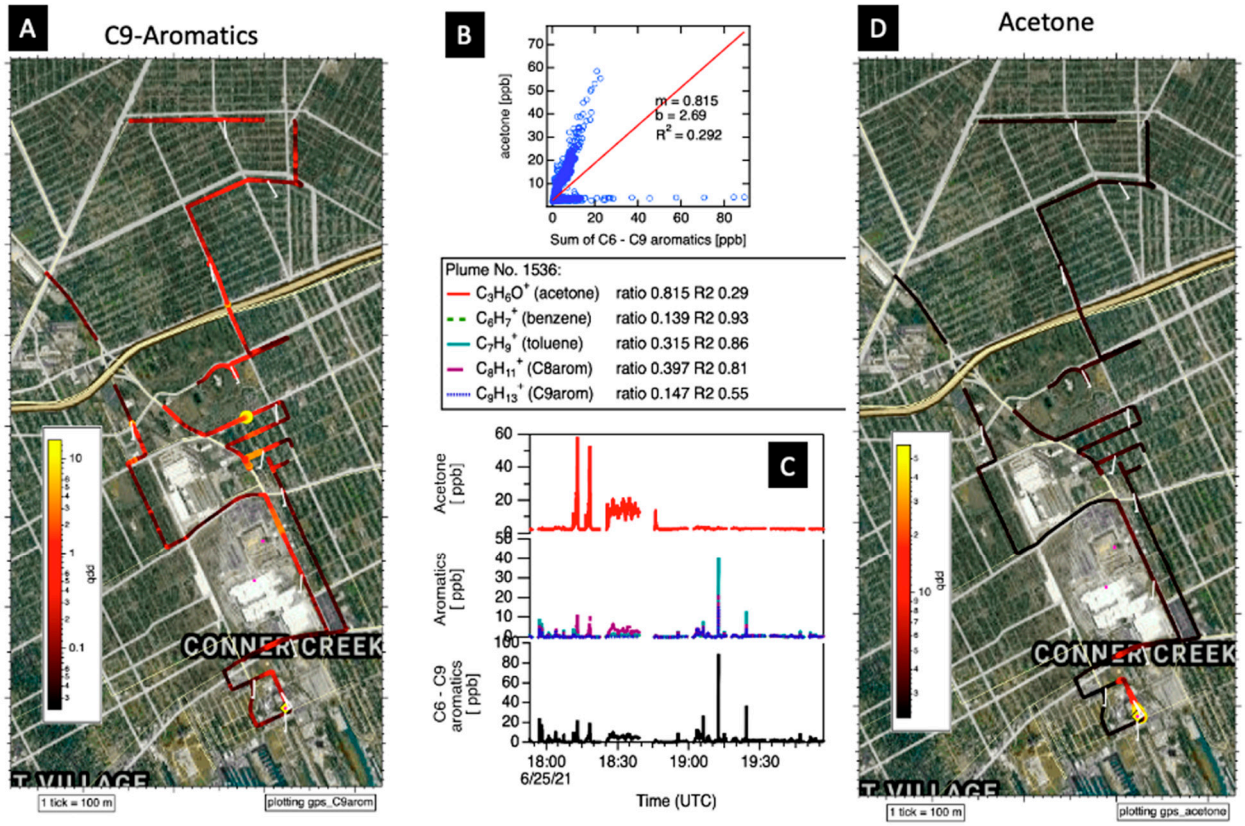

Figure S30. Mixed plume from chemical waste site WA236, and other nearby sources. Image source: Google Maps. Imagery ©2023 Airbus, CNES/Airbus, First Base Solutions, Landsat / Copernicus, Maxar Technologies, Sanborn, U.S. Geological Survey, USDA/FPAC/GEO.

WA236 was quantified slightly further downwind, in order not to saturate the instrument. Figure S26 shows a GC of one such period. Notable enhancements of halocarbons, primarily dichloromethane (CH_2Cl_2), aromatics and acetonitrile (CH_3CN) are observed. PCBTF, not shown since no calibration is available, is also elevated. This GC data is consistent with our knowledge of this site, which accepts and stores waste solvents and paints.

S3.4. MA171 (Natural Gas Compressor Station)

Site MA141 is a natural gas compressor station. It was visited on two days, 23-May-2021 and 15-June-2021.

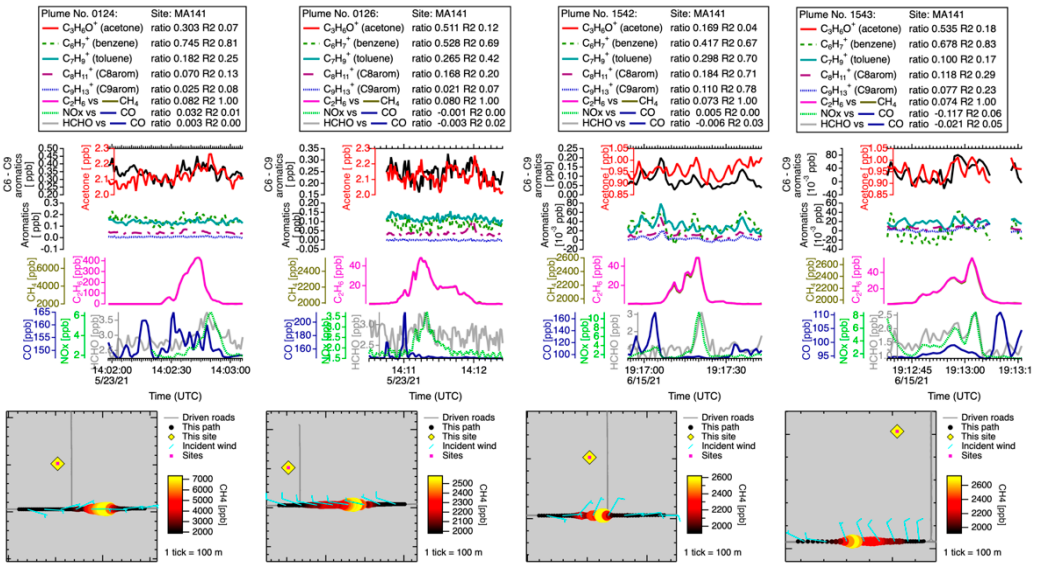

Figure S31. Plumes from MA141 compressor station on 23-May-2021 and.

S3.5. On-Site Drive: WA87 (automaker) and WA0 (steel manufacturer)

On 24-June-2021 the Aerodyne Mobile Laboratory obtained permission to drive on facility-owned roads at the automaker and steel manufacturer complex (WA87/WA0). The goal of these measurements was to allow for the emissions from the two closely nestled facilities to be separated. On-site measurements were conducted between the times of 12:38:34 and 16:18:44 UTC. Wind was from the SSE for most of the measurements, though channeling of wind between buildings was observed.

These measurements show multiple concentration enhancements (plumes) measured on facility roads. About a dozen of these plumes have been deemed distinct (originating from different emission sources). These plumes vary in chemical composition. Several mixed aromatics plumes, for example, were measured in the northern section of the complex (WA87). These plumes could be distinguished by varying contributions of xylenes or C9-aromatics like trimethylbenzene to the total. Other plumes measured at the east of the facility (WA0) contained combustion tracers like carbon monoxide and carbon dioxide. One such plume also contained NOx and formaldehyde. Another contained natural gas; it may be due to a neighboring power generation facility. To the south-west of the facility, a mixed VOC plume was observed, containing oxygenated VOCs like acetone, methyl ethyl ketone or butanal. A summary of observed plumes by location is shown in the figure below.

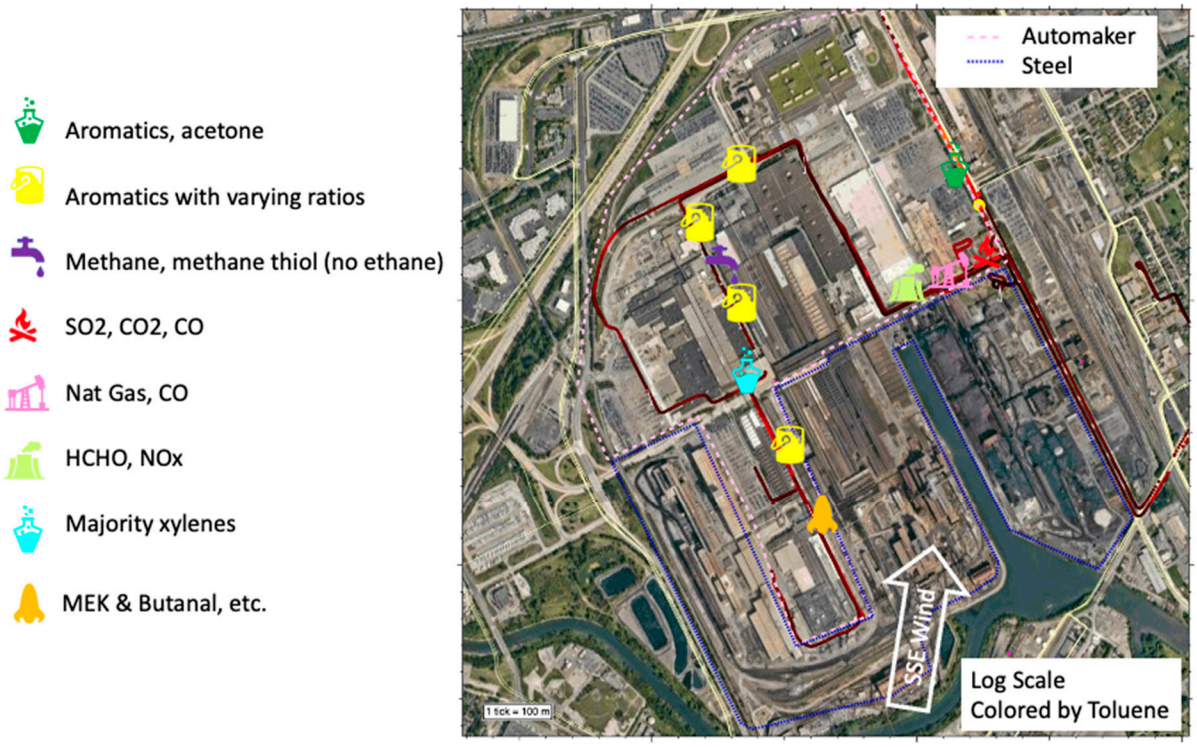

Figure S32. Summary sources for the WA87/WA0 site drive (plume 1510). The driven path is colored by toluene concentration (log scale, blue to pink). The distinct plumes noted are indicated by colored icons. Image source: Google Maps. Imagery ©2023 Airbus, CNES/Airbus, Maxar Technologies, Sanborn, U.S. Geological Survey, USDA/FPAC/GEO.

Two example aromatic plumes with differing fingerprints from WA87 are shown in Figure S33 below. The first plume contains significant C9-aromatics and was measured closest to a "Body Shop" building. The second plume (right) has proportionally more toluene and C8-aromatices (xylenes) and less C9-aromatics and was measured closer to the "Stamping Plant" building.

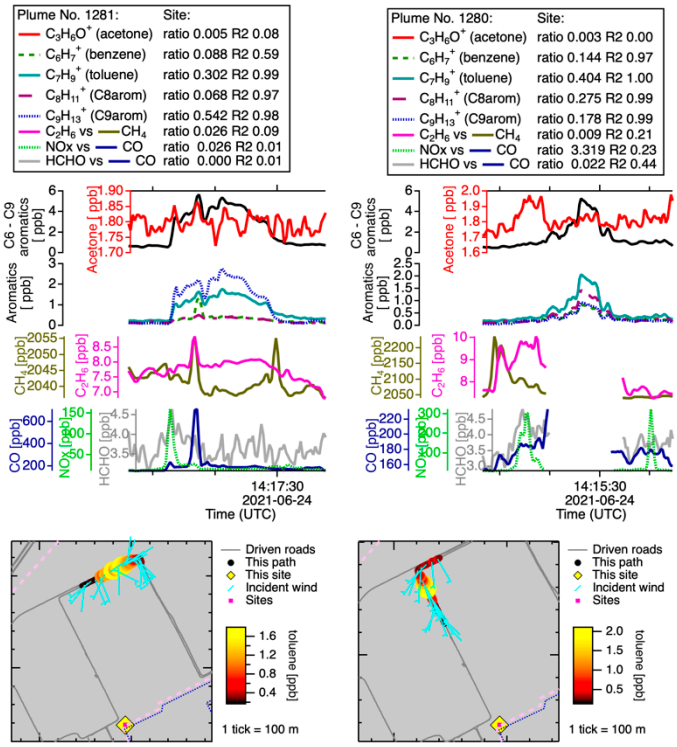

Figure S33. Example of WA87 plumes with distinct aromatic ratios.

Several stationary GC measurements were also taken throughout the facility. These measurements allow us to identify any additional enhanced VOCs, and are particularly useful in speciating the larger aromatics species. For example, Figure S34 shows a stationary GC taken near the "Tool & Die Plant". Toluene and the C9-aromatics are elevated. The GC identifies that the C9-aromatics are dominated by 1,2,4-trimethylbenzene. We note that this measurement was taken on the border between WA87 and WA0 and it is not possible to definitively attribute this plume to one or the other.

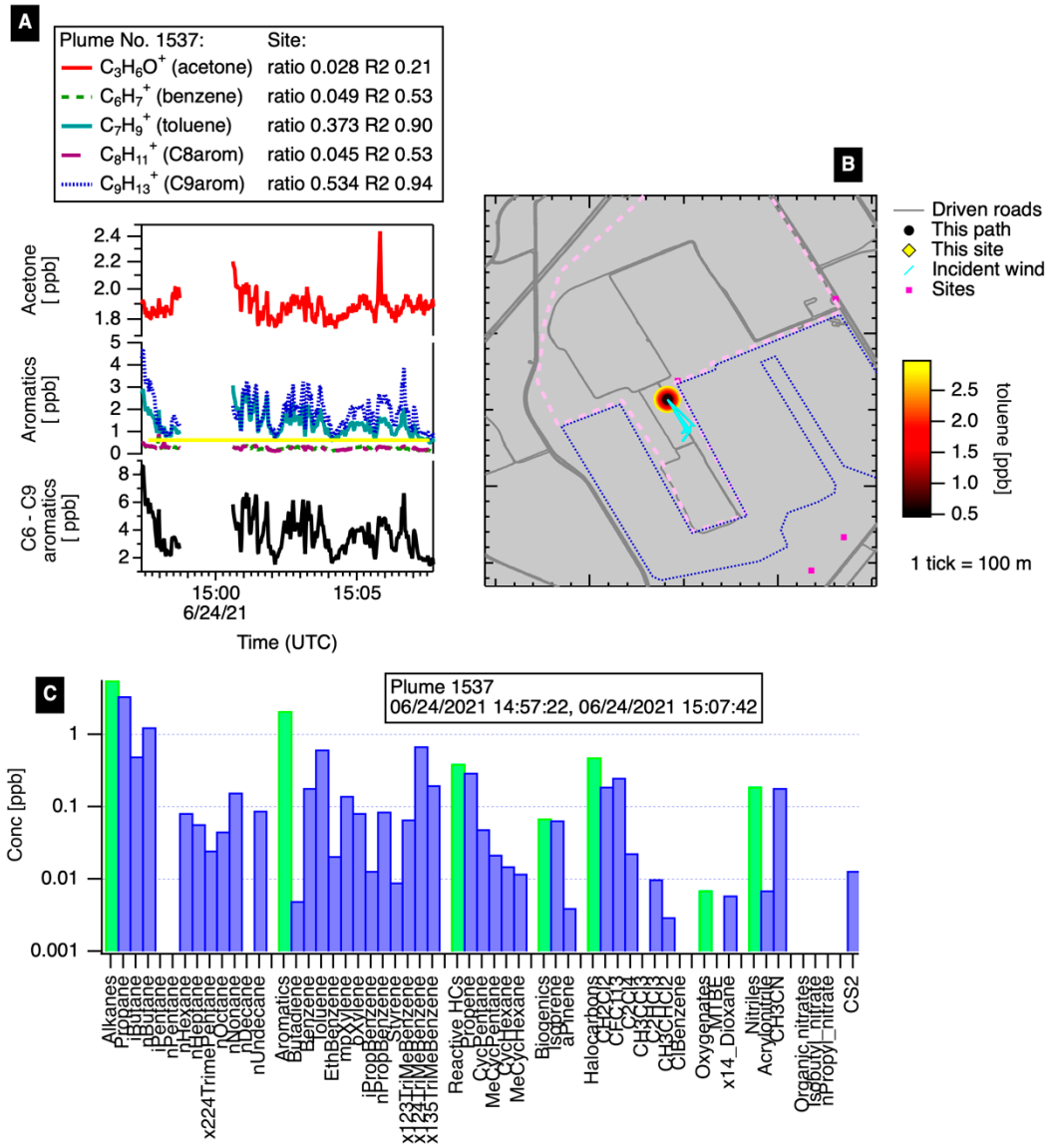

Figure S34. Stationary GC measurement on the border between WA87 (pink dashed outline) and WA0 (blue dotted outline).

In contrast, a stationary GC taken further south, in between the "Engine/Fuel Tank Plant" and the "Stamping Plant" shows emissions dominated by C8-aromatics. The GC finds the xylenes to be predominantly m- and p-xylenes (the two are quantified together in the GC) as opposed to o-xylene or ethylbenzene (Figure S35).

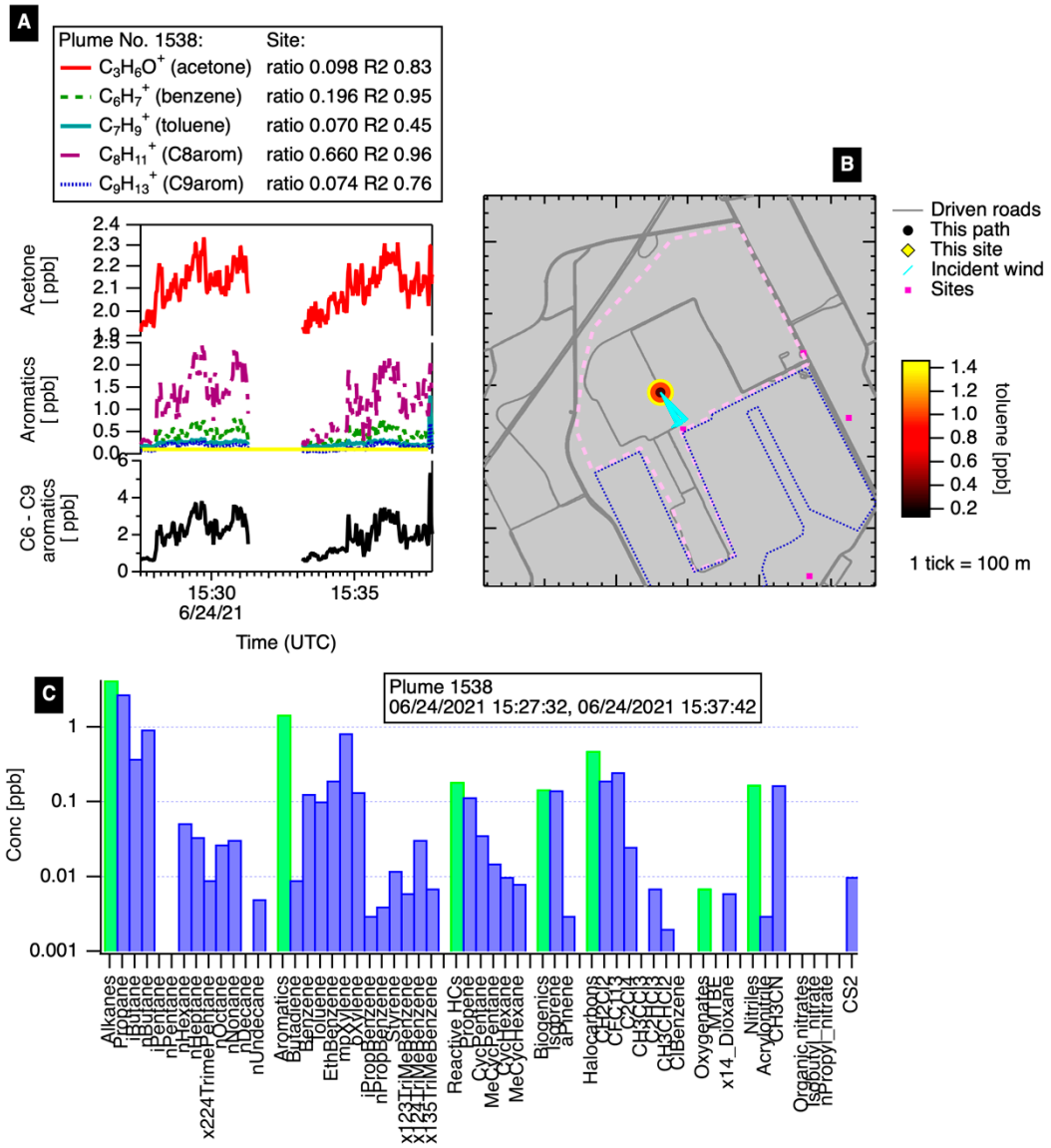

Figure S35. Stationary GC in between the WA87 "Engine/Fuel Tank Plant" and the "Stamping Plant." Facilities WA87 (pink dashed outline) and WA0 (blue dotted outline) are drawn.

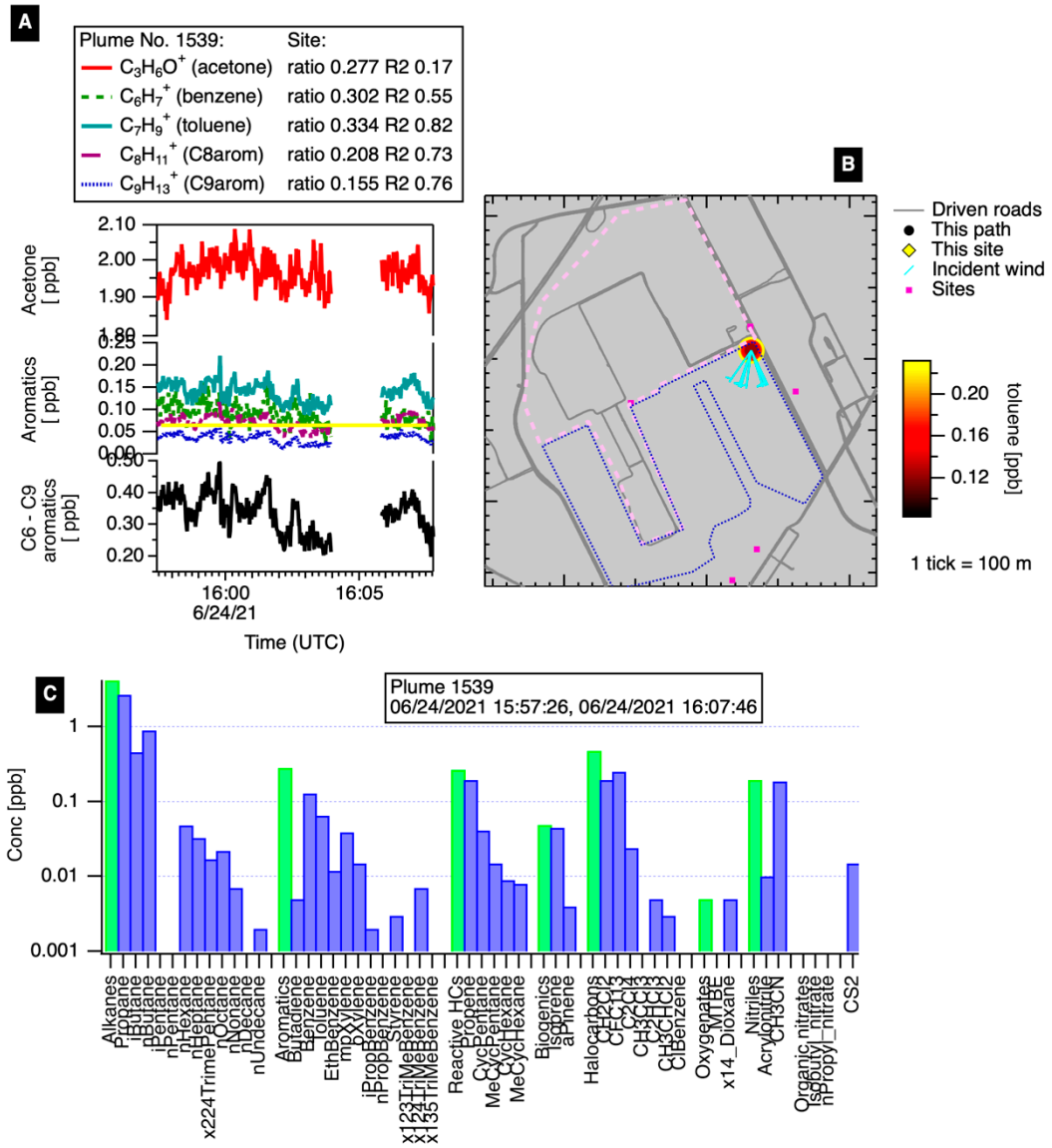

Figure S36. A stationary GC taken downwind of WA87 (pink dashed outline) and WA0 (blue dotted outline).

A stationary GC was taken downwind of WA0 (Figure S36). This GC shows low levels of aromatics and most other VOCs. Examining the full time series (Figure S37), we see enhancements of combustion tracers, notably CO. These enhancements are somewhat correlated with ethane and methane. Separate correlated enhancements of CO_2 and NOx are also observed. SO_2 is also enhanced during this period, though the slower sampling time of this instrument makes it difficult to associate the SO_2 with either CO or the CO_2 plumes. We note that Dearborn Industrial Power Generation is located near to this sampling spot, and could be contributing to these emissions, particularly the ethane/methane/CO plumes.

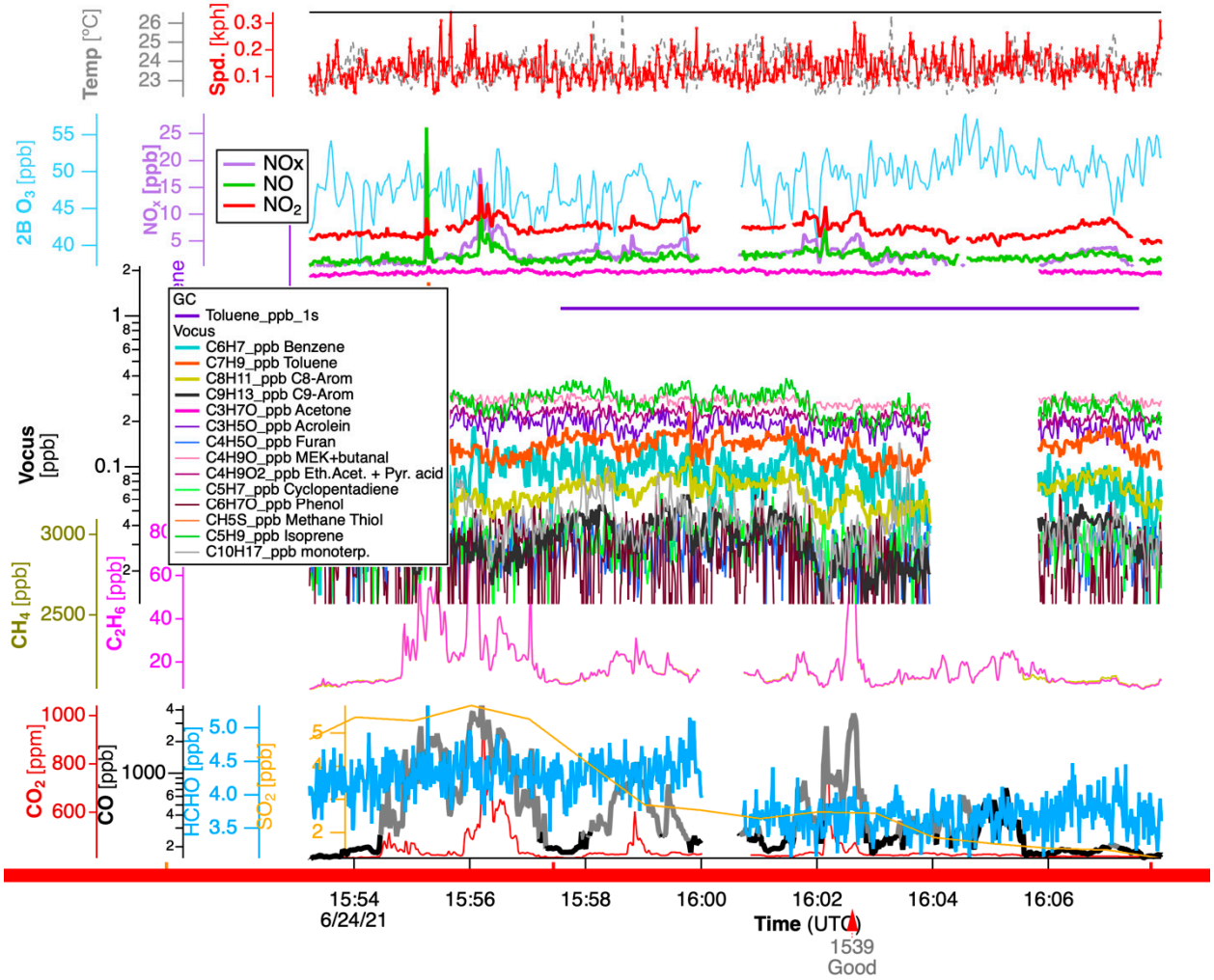

Figure S37. Full time series of 1-second tracers covering the GC period (purple horizontal line) shown in Figure S36.

One example of a formaldehyde plume measured at this complex is shown below (Figure S38). This plume shows correlated enhancements of HCHO, CO_2 and NOx. CO may also be slightly correlated, though an overlapping ethane/methane/CO source obscures most features. Background formaldehyde concentrations were elevated on this day (~4 ppb) and rise to ~8 ppb in this plume. Scientists noted rail cars containing molten steel nearby.

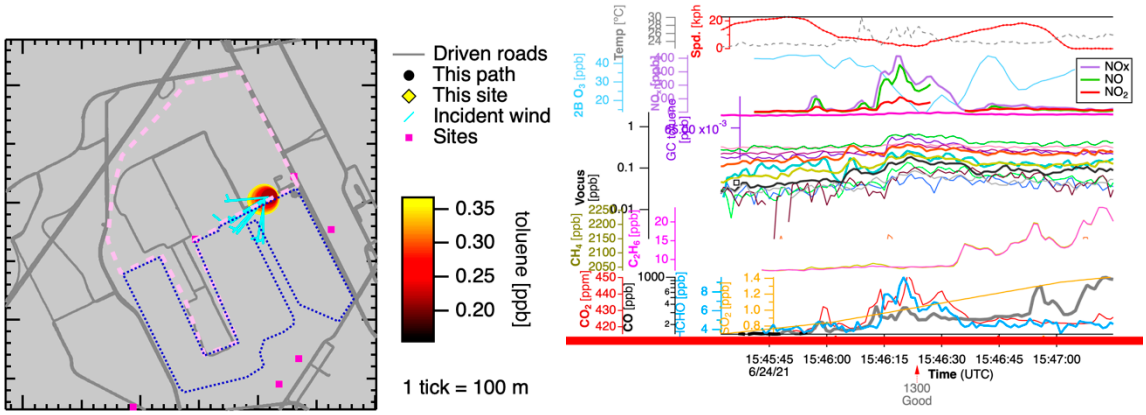

Figure S38. Example formaldehyde plume observed at the border of WA87 (pink dashed outline) and WA0 (blue dotted outline). HCHO (blue) is correlated to NOx (purple) and CO_2 (red).

S3.6. On-Site Drive: WA22 (refinery)

Site WA22 is a refinery located in Wayne County Michigan. This site processes crude oil into gasoline and various other products for distribution (including propane and additional petrochemicals). As of 2021, it was the only active petroleum refinery in Michigan. Sections of the site include a tank farm, refinery operations, multiple specialized plants, and an asphalt terminal. In 2020, the EPA reported air releases of benzene (5,914 lbs.), toluene (9,966 lbs.), 1,3-butadiene (1,545 lbs.), C_8 (xylene isomers and ethylbenzene, 11,735 lbs. combined), and C_9 (1,2,4-trimethylbenzene and cumene, 3,405 lbs. combined) aromatics from the WA22 facility as part of the Toxics Release Inventory Program. Some other chemicals reported include hydrogen cyanide, ammonia, and hydrogen sulfide.

On-site measurements at WA22 were conducted on 29-June-2021 between 14:18 UTC and 17:05 UTC. During this visit to the refinery, the AML conducted mobile and stationary sampling near the delayed coker unit, hydrogen plant, asphalt terminal area and tank farm. Various solvent and BTEX species were observed at different locations with and without combustion and natural gas tracers. Wind direction was generally favorable towards isolating emissions from the facility but other on-site operations (e.g. diesel trucks) did present potential interferences. In all, the AML conducted three hours of largely mobile surveying at the facility along with occasional stationary GC cycles.

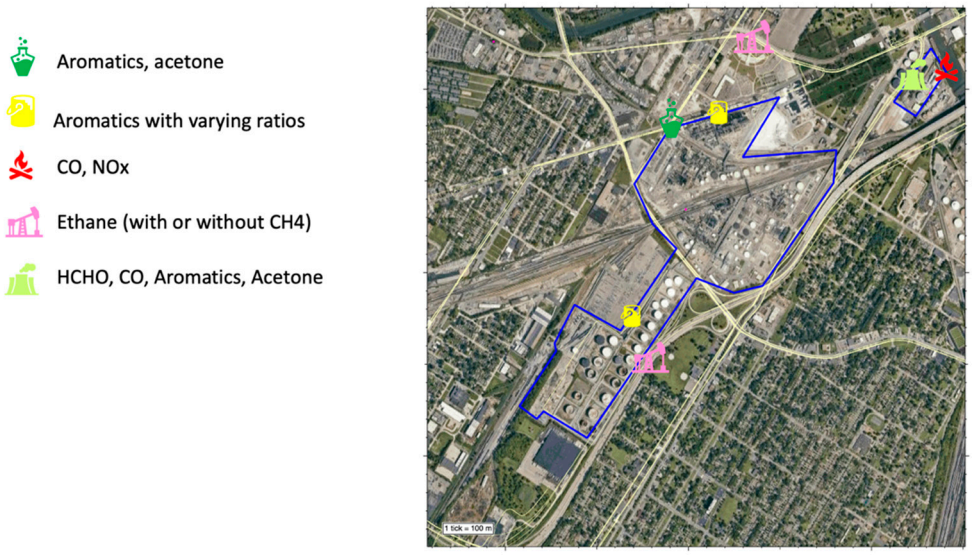

Figure S39. WA22 facility boundaries (blue) showing satellite underlay and symbols indicating observed plume types. Image source: Google Maps. Imagery ©2023 Airbus, CNES/Airbus, Landsat / Copernicus, Maxar Technologies, Sanborn, U.S. Geological Survey, USDA/FPAC/GEO.

Petroleum Coke Processing area

Several sampling transects along the northern border road were conducted with the AML between 14:18 – 14:38 UTC. Wind direction and speed varied, with operators noting SW and WSW winds with moderate strength based on facility windsocks or flags. Along the northern facility fencline in the general area of the delayed coker unit and hydrogen plant a 30-second enhancement of C_6-C_9 aromatic VOCs (Figure S40) was measured, containing peaks between 0.69 ppb (benzene) and 2.0 ppb (toluene).

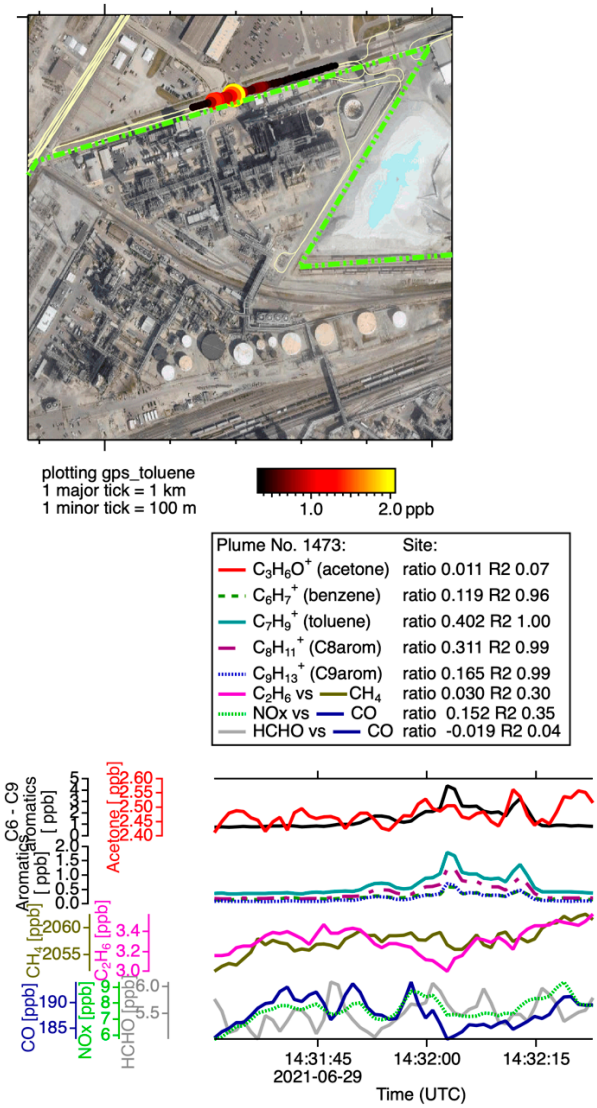

Figure S40. Mobile measurement downwind of WA22 refinery 29-June-2021. Map (left panel) colored by toluene ($C_7H_9^+$) and time series (right panel) of C_6 – C_9 aromatics and acetone (Plume 1473, 14:31 – 14:32 UTC). See legend for aromatic compounds in Figure S33. Image source: Google Maps. Imagery ©2023 Airbus, CNES/Airbus, Maxar Technologies, Sanborn, U.S. Geological Survey, USDA/FPAC/GEO.

Persistent enhancements of toluene and acetone were observed along the northern facility boundary during multiple short (1-minute) stationary periods in a SW wind absent of vehicle combustion markers or other notable aromatics (benzene, C_8- and C_9-aromatics). See example in Figure S41. No clear source of the solvents could be identified. A GC cycle that occurred between 14:50 – 15:00 UTC, while stationary in this area, was dominated by alkanes (propane, butane; ~2 ppbv sum) but previously observed compounds were not present at the time.

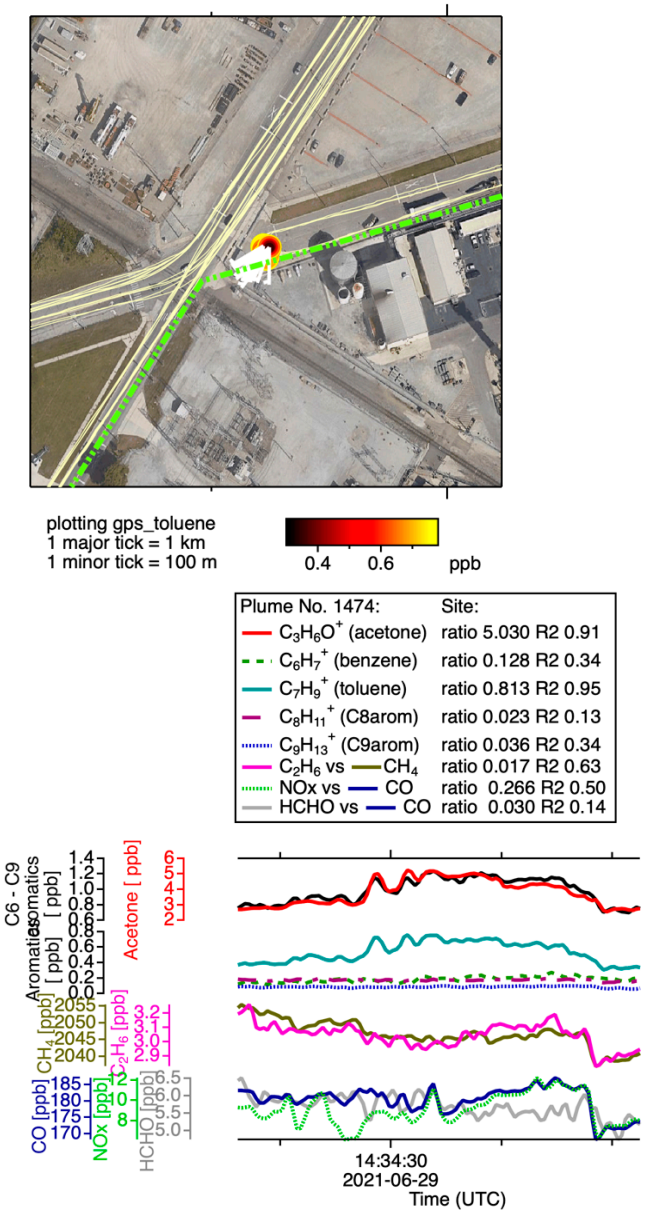

Figure S41. Stationary measurement downwind of WA22 refinery in Detroit on 29-June-2021. Satellite map (left panel) colored by toluene ($C_7H_9^+$) and time series (right panel) of C_6 – C_9 aromatics and acetone shown with correlation analysis relative to the summed aromatics traces (Plume 1474, 14:33 – 14:36 UTC). Image source: Google Maps. Imagery ©2023 Airbus, CNES/Airbus, Maxar Technologies, Sanborn, U.S. Geological Survey, USDA/FPAC/GEO.

Surrounding roads

During multiple passes in front of WA22, short-lived spikes of natural gas (5.5 – 7.5% C_2H_6:CH_4) were observed consistently near a driveway in the same location (see example in Figure S42). Possible emission vectors could be underground access points (manholes) in the road venting infrastructural leaks (city distribution) through the sewer system or soil.

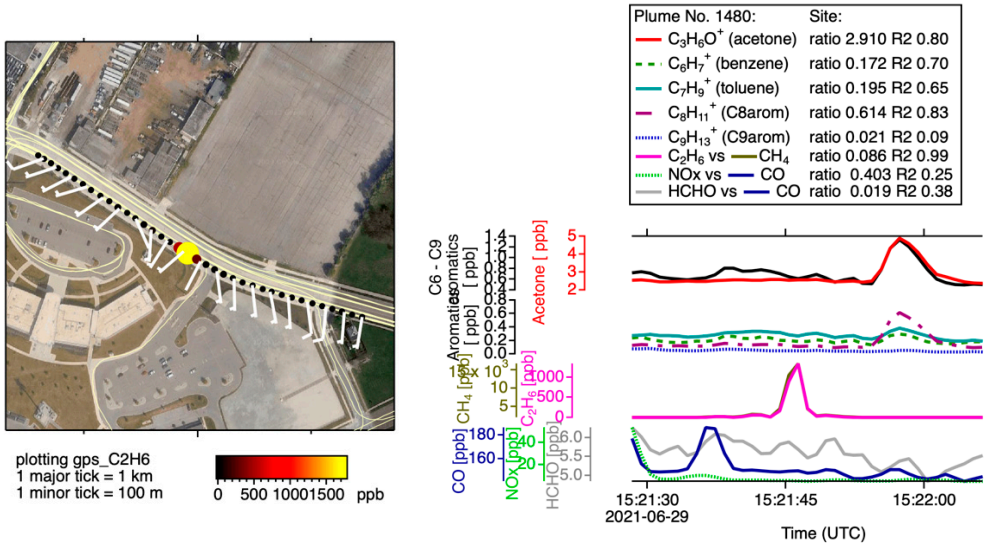

Figure S42. Time series of ethane and methane concentration during a driven transect. Image source: Google Maps. Imagery ©2023 Airbus, CNES/Airbus, Maxar Technologies, Sanborn, U.S. Geological Survey, USDA/FPAC/GEO

Asphalt Terminal area

At 15:20 UTC, the AML began driving to the asphalt terminal. After a short drive, a spike of HCHO (59 ppb) was measured along with several other compounds when passing storage tanks (see orange star in Figure S43; Plume 1482, 15:24 – 15:25). A more prolonged plume of similar composition occurred while on Stocker St and continued after turning onto the asphalt terminal property (Figure S43). Wind speed and direction were weak, limiting potential source attribution. Other potential sources near this location include the a warehouse with multiple industries including metals, recycling and engine parts.

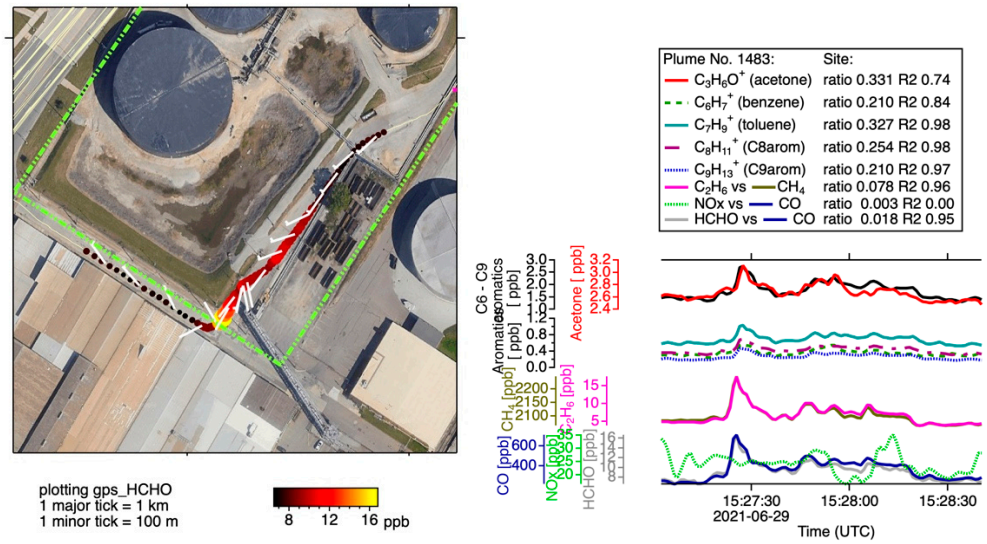

Figure S43. Mobile measurement in the area of the WA22 asphalt terminal on 29-June-2021 (Plume 1483, 15:26 – 15:29 UTC). Satellite map (top left panel) colored by formaldehyde (HCHO). Time series (right) of select VOCs and trace gases. Image source: Google Maps. Imagery ©2023 Airbus, CNES/Airbus, Maxar Technologies, Sanborn, U.S. Geological Survey, USDA/FPAC/GEO.

Between 15:30 – 16:00 UTC, the AML sat stationary along the fenceline near the river in a corner of the terminal area. Several trucks were also moving in and out of the area. Site operators indicated that a nearby building, periodically emitting dark smoke and a

strong odor, served the housing for the hot oil heaters. At 15:30 UTC, the AML encountered a plume containing benzene, CO, NO_x, and CH_4, absent of C_7 – C_9 aromatics, C_2H_6, or HCHO (Figure S44). A similar plume occurred a couple minutes later after stopping at the fenceline, now containing additional species, C_7 – C_9 aromatics and acetone, but negligible C_2H_6 and HCHO. Wind direction shifted back and forth within the SW quadrant for the duration of the stationary period, moving across most parts of the terminal area at one point or another. For the remaining time at this location (15:35 – 16:00 UTC), wind shifted back and forth between two types of plumes, one primarily consisting of solely NO_x and another of C_7 – C_9 aromatics and acetone.

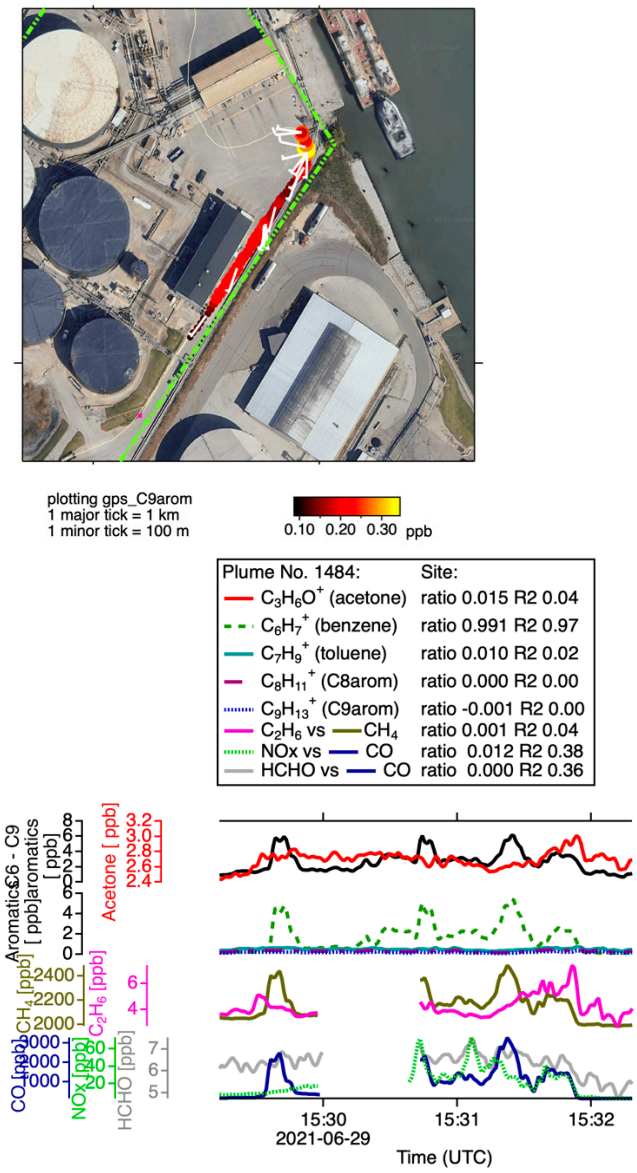

Figure S44. Mobile and stationary measurements in the area of the WA22 asphalt terminal on 6/29/2021 (Plume 1484, 15:30 – 16:00 UTC). Satellite map (left) colored by C9-aromatics. Time series (right) of select VOCs and trace gases. Image source: Google Maps. Imagery ©2023 Airbus, CNES/Airbus, Maxar Technologies, Sanborn, U.S. Geological Survey, USDA/FPAC/GEO.

Crude Processing Facility and Tank Farm area

At 16:00 UTC, the AML parked in a lot near the crude processing facility. While stationary, a GC cycle was completed. Wind direction was narrowly focused out of the SW without much spread over the 20 minute period. A notable enhancement of $C_5H_9^+$ and

small enhancements of C_6 – C_9 aromatics were observed with C_2H_6 and CH_4 (two different regimes of C_2H_6:CH_4 ratios, 16:10 – 16:18 UTC: 4%; 16:20 – 16:30 UTC: < 1 %).

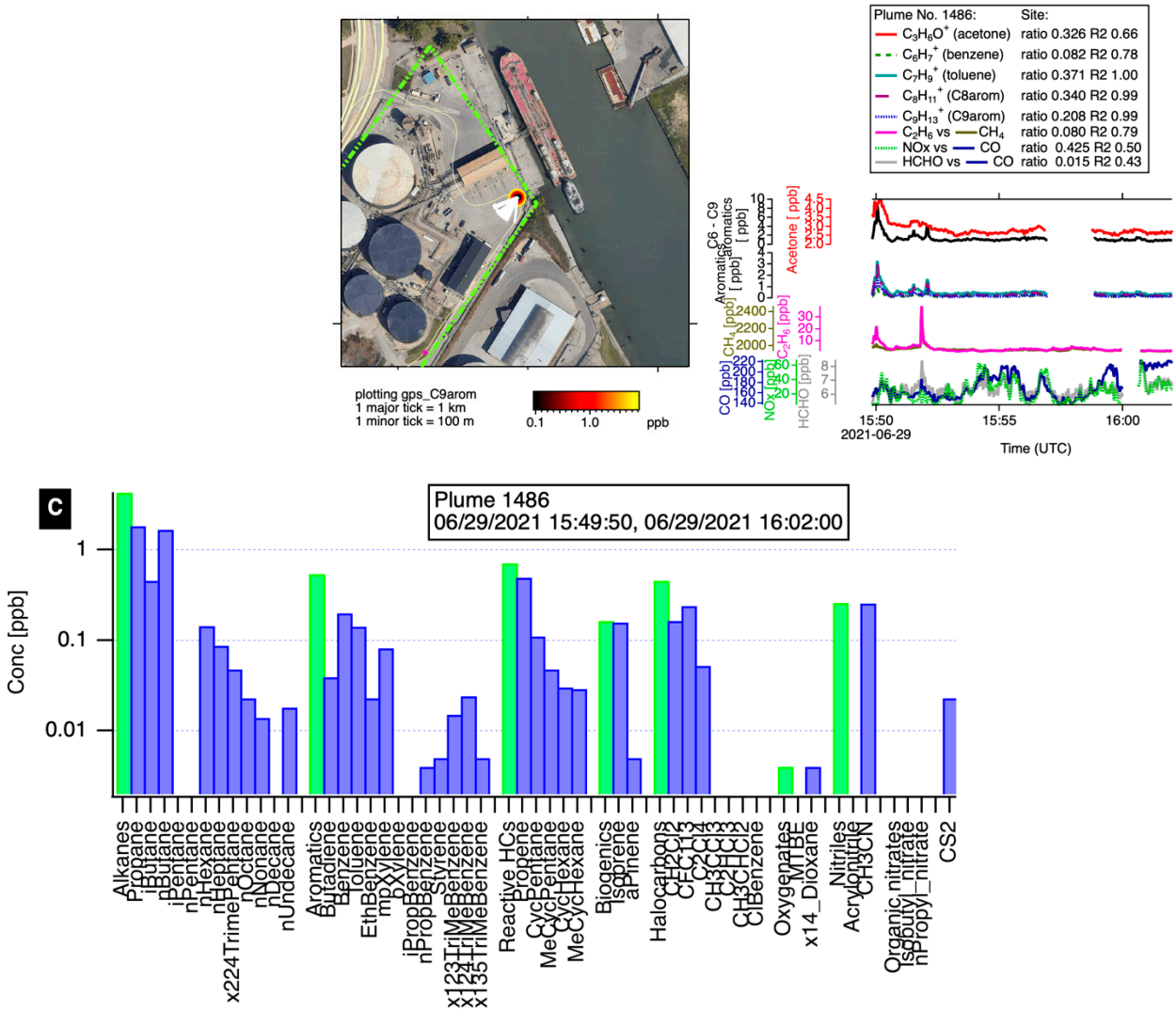

Figure S45. Plume 1486. Stationary measurements at the tank farm. Image source: Google Maps. Imagery ©2023 Airbus, CNES/Airbus, Maxar Technologies, Sanborn, U.S. Geological Survey, USDA/FPAC/GEO.

At 16:35 UTC, the AML went to the tank farm southwest of the WA22 facility. Most tanks contained crude oil, some with gasoline or butane. During a looping drive around the tanks on the eastern end, ethane concentration increased without methane present for 1 minute at 16:38 UTC while passing 4 – 5 tanks (Figure S47)

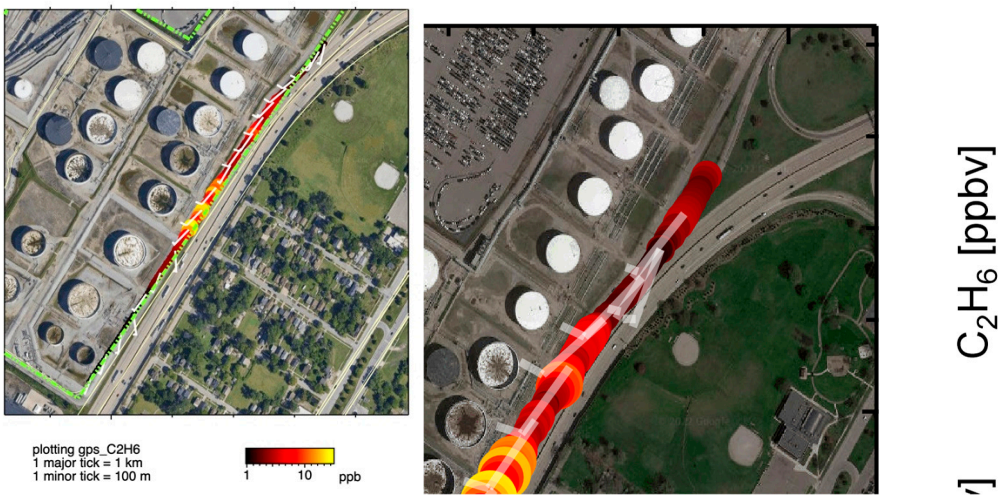

Figure S46. Mobile measurements at the eastern end of the WA22 tank farm area on 6/29/2021 (16:37 – 16:40 UTC). Satellite map (left panel) colored by C_2H_6 and time series (right panel) of ethane (C_2H_6) and methane (CH_4). Image source: Google Maps. Imagery ©2023 Airbus, CNES/Airbus, Maxar Technologies, Sanborn, U.S. Geological Survey, USDA/FPAC/GEO.

While stationary between 16:50 – 17:00 UTC, three plumes containing BTEX compounds were sampled in a SW wind, pointed towards the middle section of the west end of the tank farm. These enhancements of C_6 – C_9 aromatics were not accompanied by combustion species (NO_x, CO, etc.) or acetone (Figure S47) and lasted for 1 – 2 minutes at a time. At 17:05 UTC, the AML left the facility and returned to base.

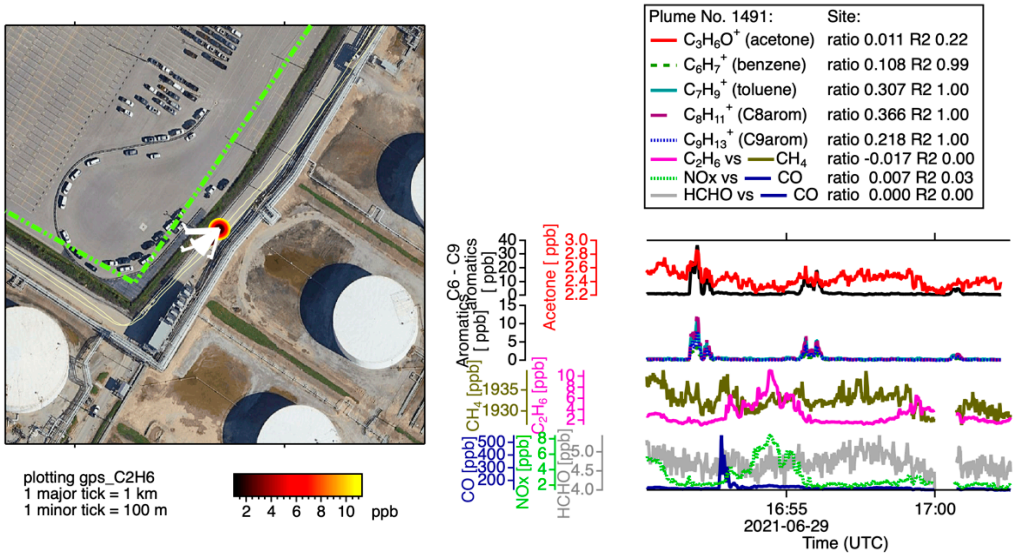

Figure S47. Stationary measurements in the WA22 tank farm area on 6/29/2021 (16:50 – 17:00 UTC). Satellite map (left panel) colored by C2H6 and time series (right panel) of C6 – C9 aromatics and acetone. Google Maps. Imagery ©2023 Airbus, CNES/Airbus, Maxar Technologies, Sanborn, U.S. Geological Survey, USDA/FPAC/GEO.

S4. Dearborn Map Averages

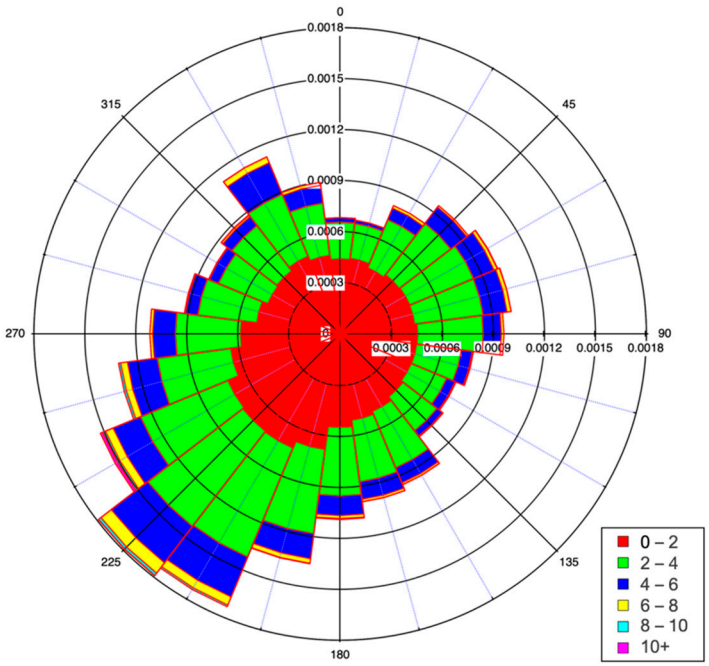

Figure S48. AML wind rose plot during "Dearborn Loop" drives.

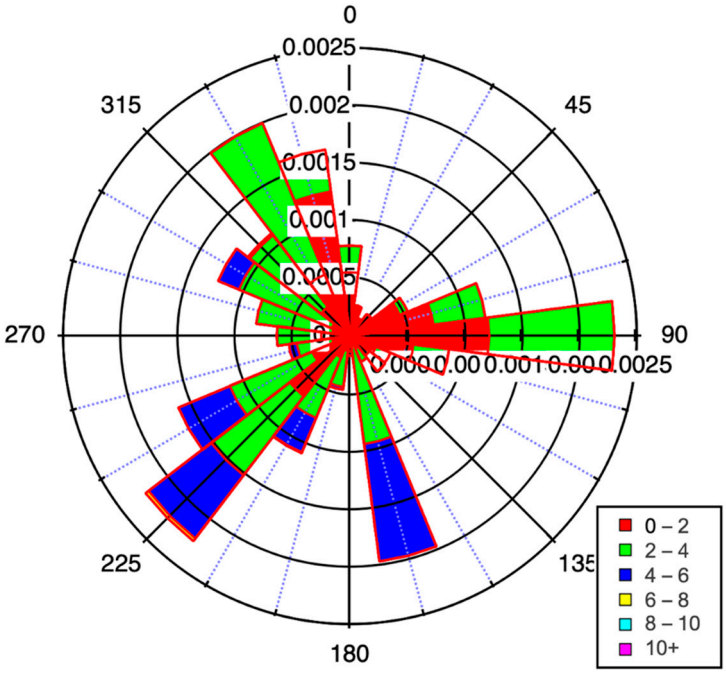

Figure S49. Dearborn Station wind rose plot during "Dearborn Loop" drives.

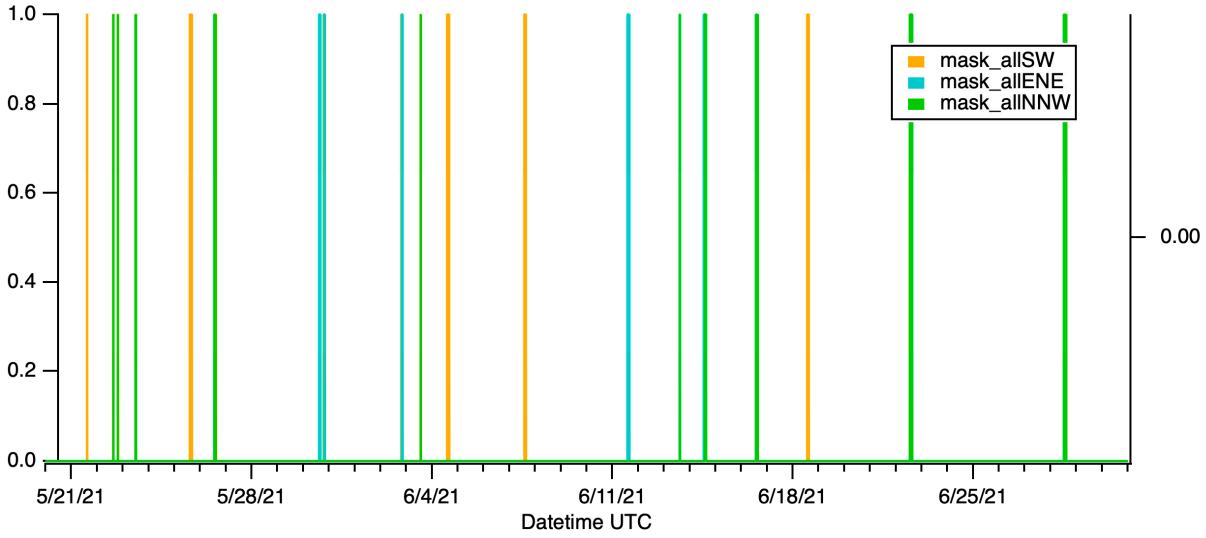

Figure S50. Overview of Dearborn Loop time periods, colored by wind direction.

S4.1.1 Sum of Aromatics Average Loop Concentrations

Bin size is 0.001 decimal degrees. The entire Dearborn Loop spans approximately 8.2 square kilometers.

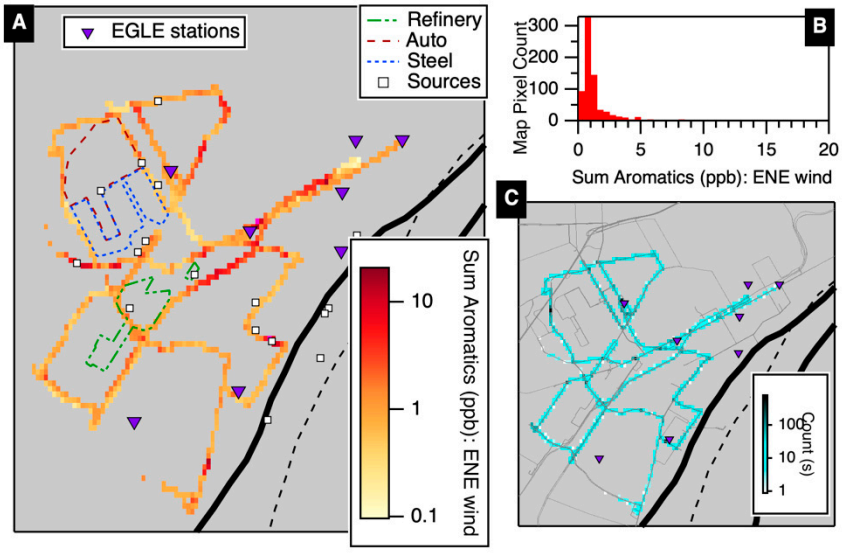

Figure S51. Average sum of aromatics (C6-C9) under winds from the ENE during "Dearborn Loop" drives (A). A histogram of the average pixel concentrations is shown, along with a map of data point counts in each bin (C).

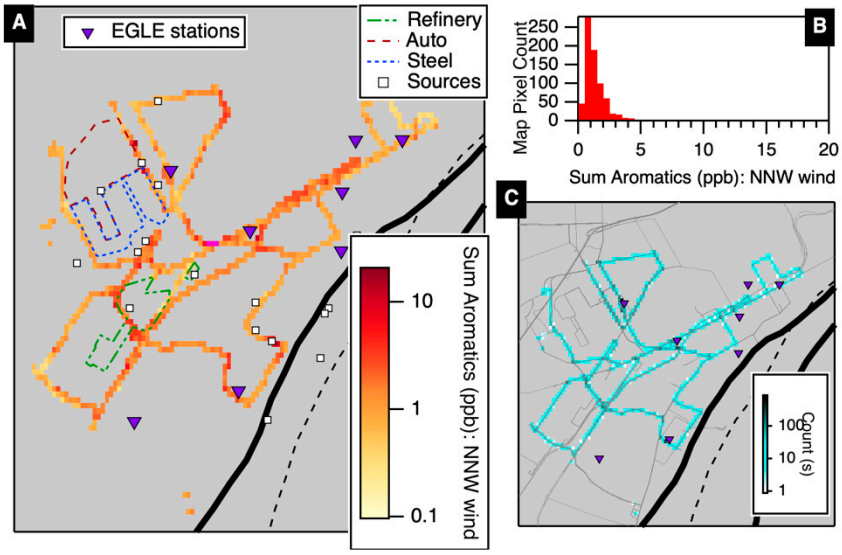

Figure S52. Average sum of aromatics (C6-C9) under winds from the NNW during "Dearborn Loop" drives (A). A histogram of the average pixel concentrations is shown, along with a map of data point counts in each bin (C).

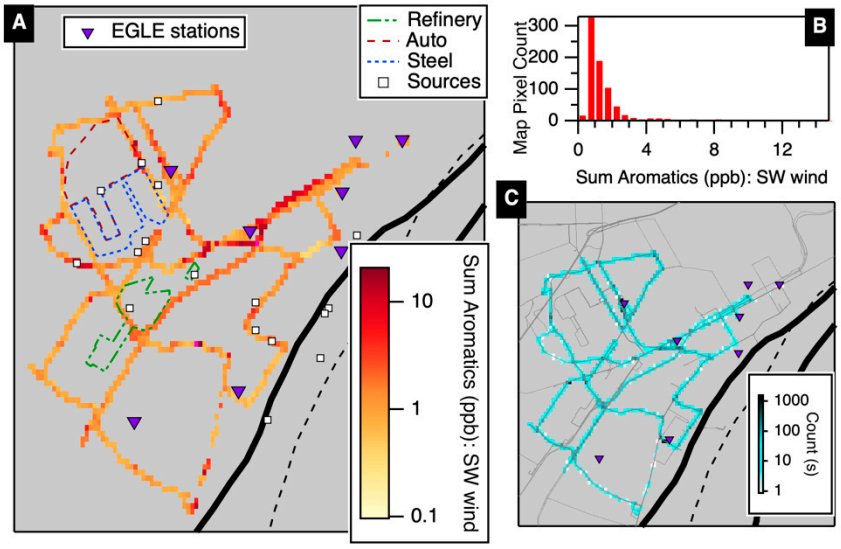

Figure S53. Average sum of aromatics (C6-C9) under winds from the SW during "Dearborn Loop" drives (A). A histogram of the average pixel concentrations is shown, along with a map of data point counts in each bin (C).

S4.1.2 Ethane Average Loop Concentrations

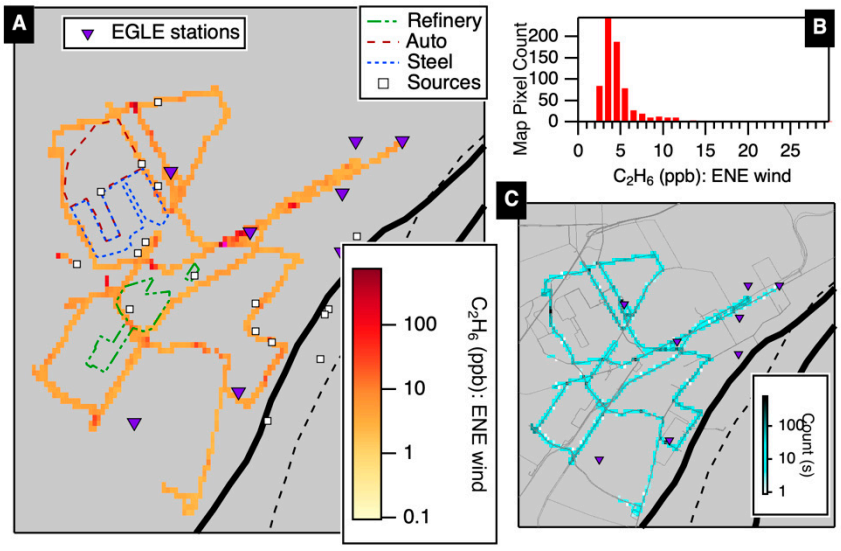

Figure S54. Average ethane concentrations under winds from the ENE during "Dearborn Loop" drives (A). A histogram of the average pixel concentrations is shown, along with a map of data point counts in each bin (C).

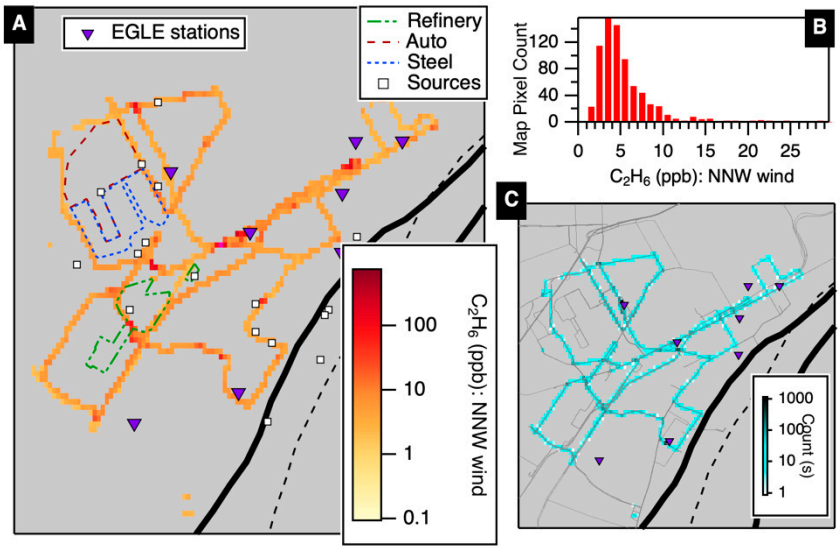

Figure S55. Average ethane concentrations under winds from the NNW during "Dearborn Loop" drives (A). A histogram of the average pixel concentrations is shown, along with a map of data point counts in each bin (C).

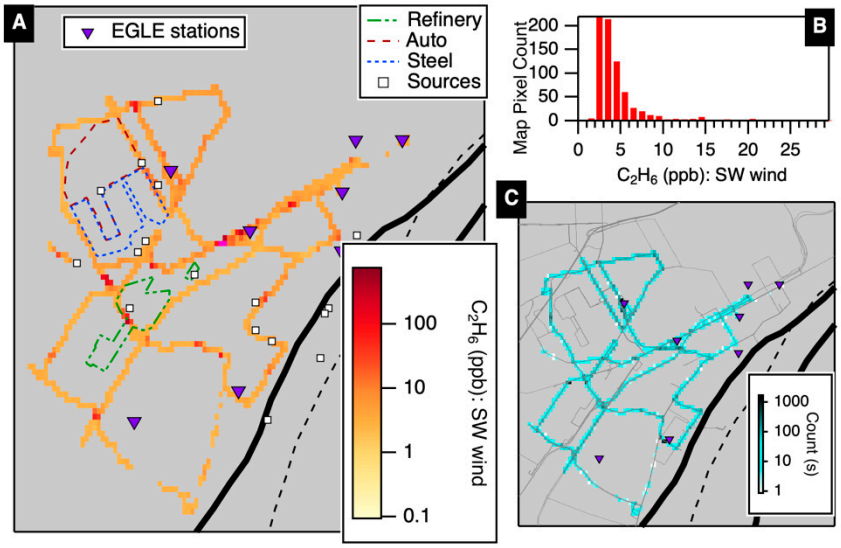

Figure S56. Average ethane concentrations under winds from the SW during "Dearborn Loop" drives (A). A histogram of the average pixel concentrations is shown, along with a map of data point counts in each bin (C).

S4.1.3 CO Average Loop Concentrations

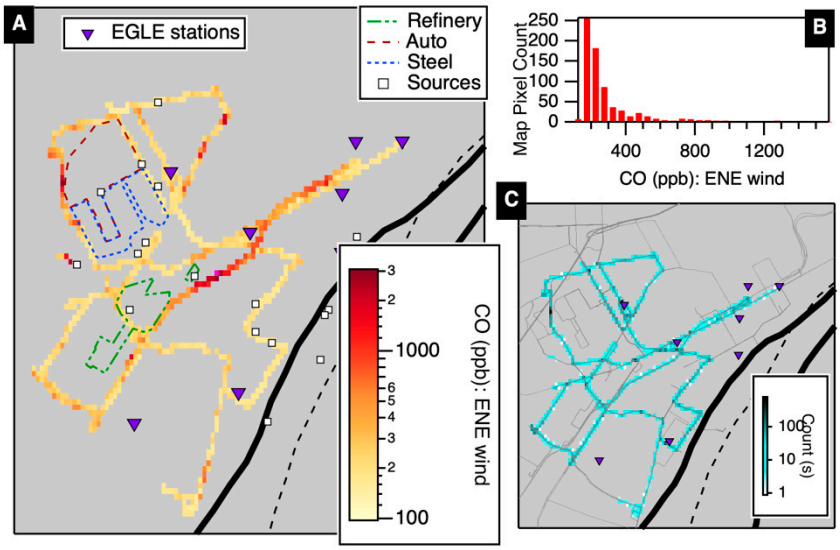

Figure S57. Average ethane concentrations under winds from the ENE during "Dearborn Loop" drives (A). A histogram of the average pixel concentrations is shown, along with a map of data point counts in each bin (C).

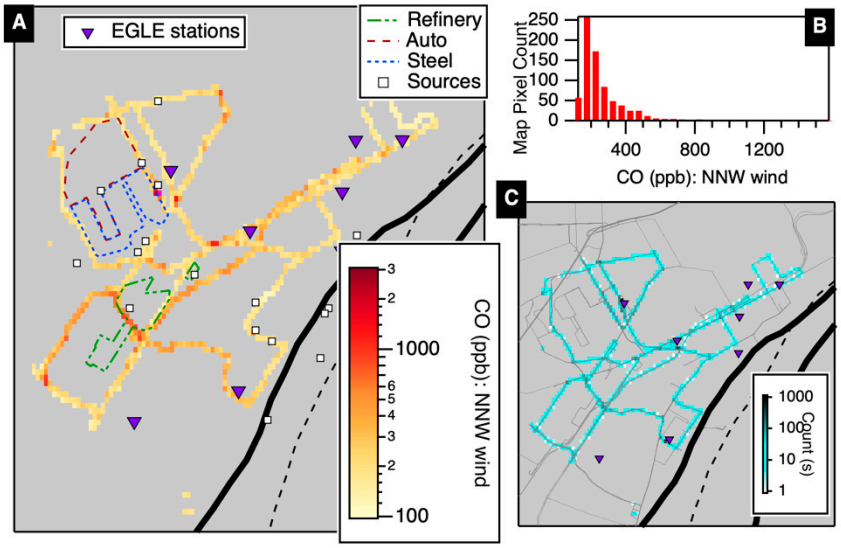

Figure S58. Average ethane concentrations under winds from the NNW during "Dearborn Loop" drives (A). A histogram of the average pixel concentrations is shown, along with a map of data point counts in each bin (C).

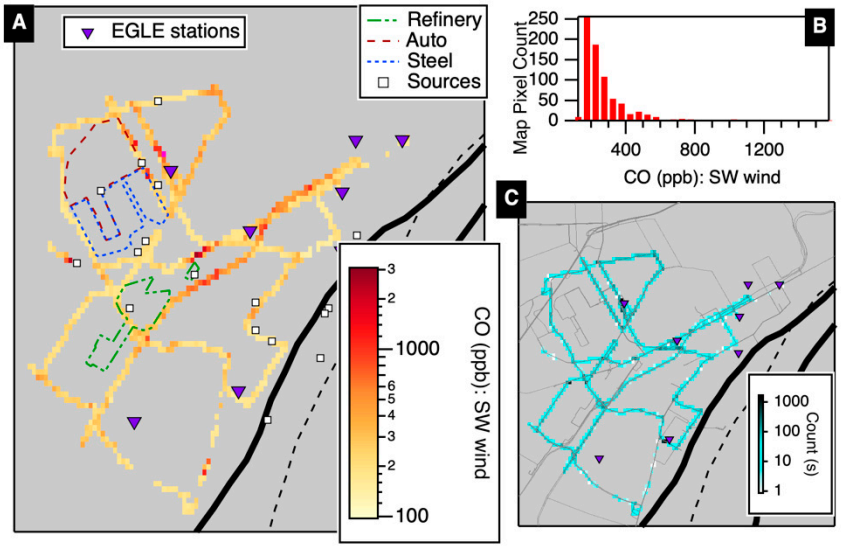

Figure S59. Average CO concentrations under winds from the SW during "Dearborn Loop" drives (A). A histogram of the average pixel concentrations is shown, along with a map of data point counts in each bin (C).

S5. Sarnia Coordinated Drive

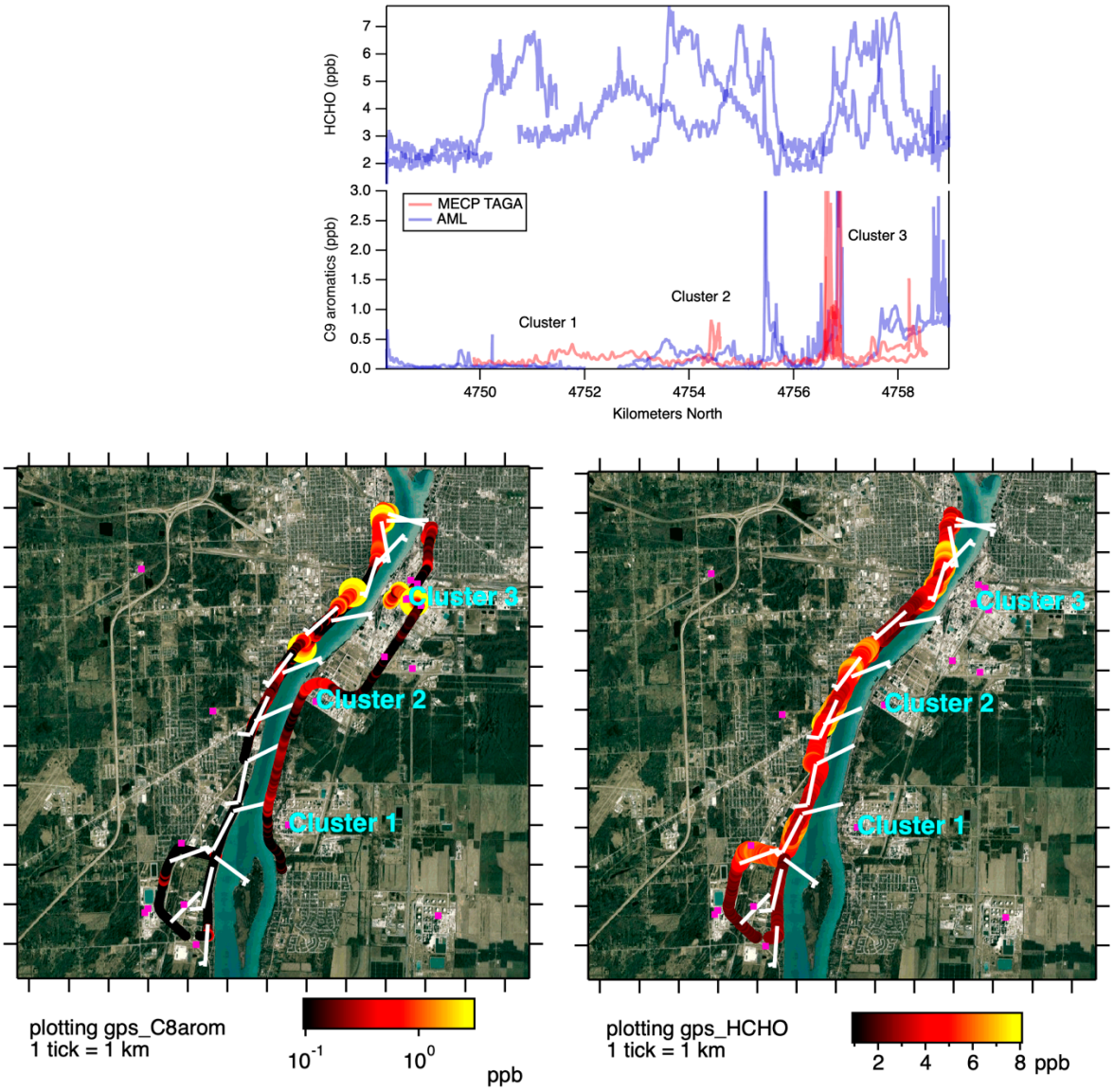

Figure S60. Coordinated River Drive between the AML (blue traces, west of river) and MECP TAGA (red trace, east of river). Mixing ratio data is plotted as a function of UTM Northing (top). Maps show C8 and HCHO. The plumes are labelled to match the clusters shown in the map. The map plots C9 aromatic concentration in log scale, with axis cut off at 3 ppb. Regional winds were generally from the NE, though local winds were impacted by the water. Satellite image source: Google Maps. Imagery ©2023 TerraMetrics.

S5.1. Additional tracers

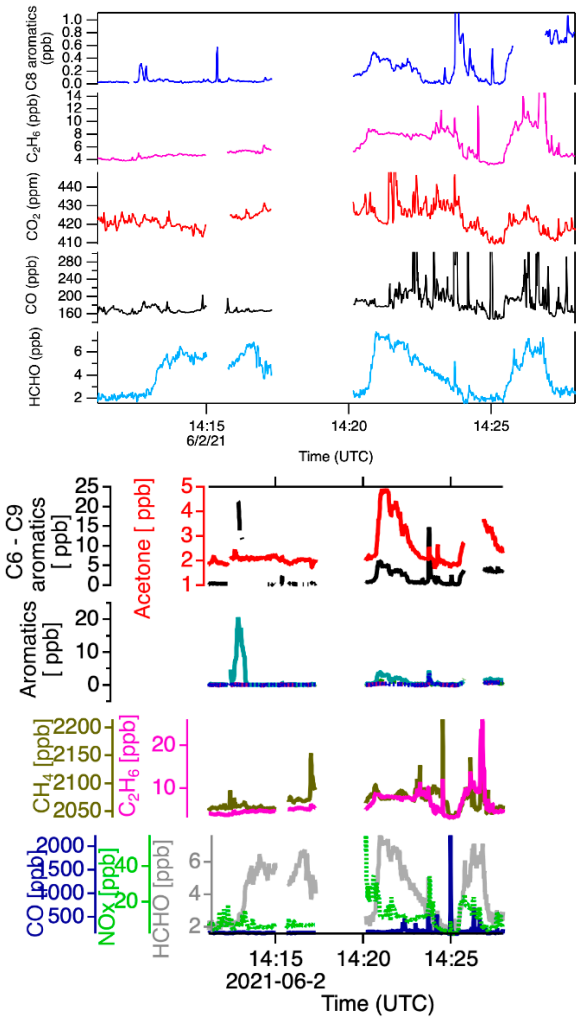

Figure S61. Additional tracers measured during a downwind transect of Canadian sites: Clusters 1, 2 and 3. Note the narrow toluene plume, which is due to site SA96.

S5.2. GC measurements

Stationary measurements downwind of refineries were done on 6/2/2021. Two stationary GC samples were taken riverside in Sarnia on 2021-6-2, with southerly winds. The first represents a background measurement, based on ethane concentrations of ~5 ppb with limited plume structure. This background shows propene at 0.176 ppb. The second shows modest plume structure in ethane, with enhancements up to 7-8 ppb. Propene is 0.59 ppb. There is not much difference between GC-measured alkanes (C3-C10) or aromatics between these two samples.

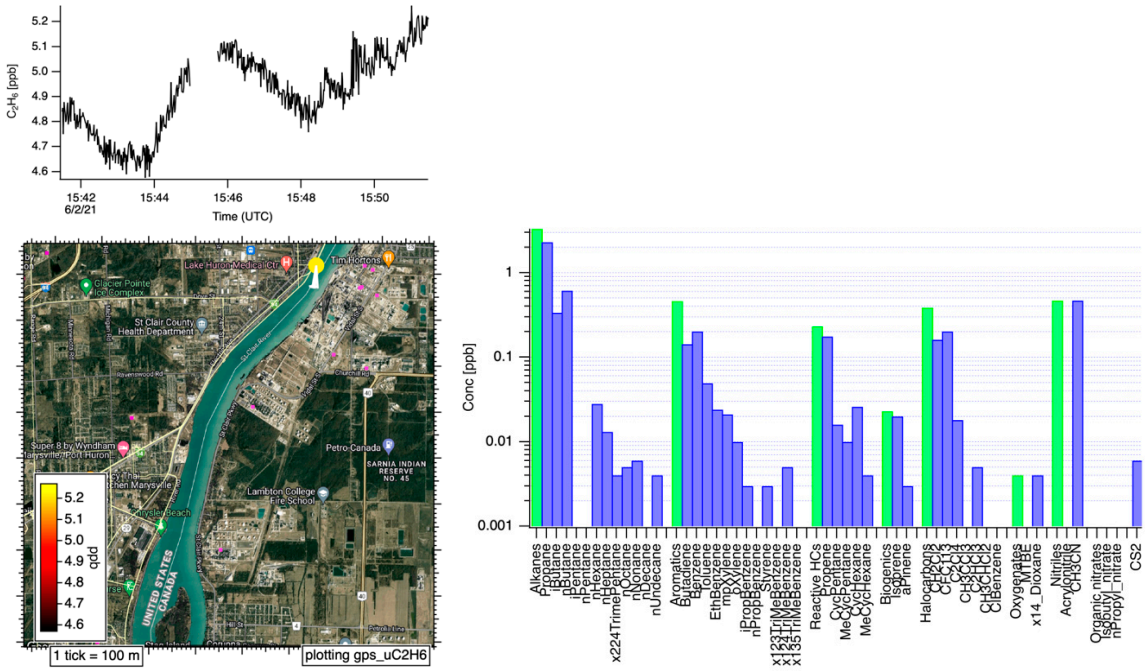

Figure S62. Background measurements showing 0.176 ppb propene. Satellite image source: Google Maps. Imagery ©2023 TerraMetrics.

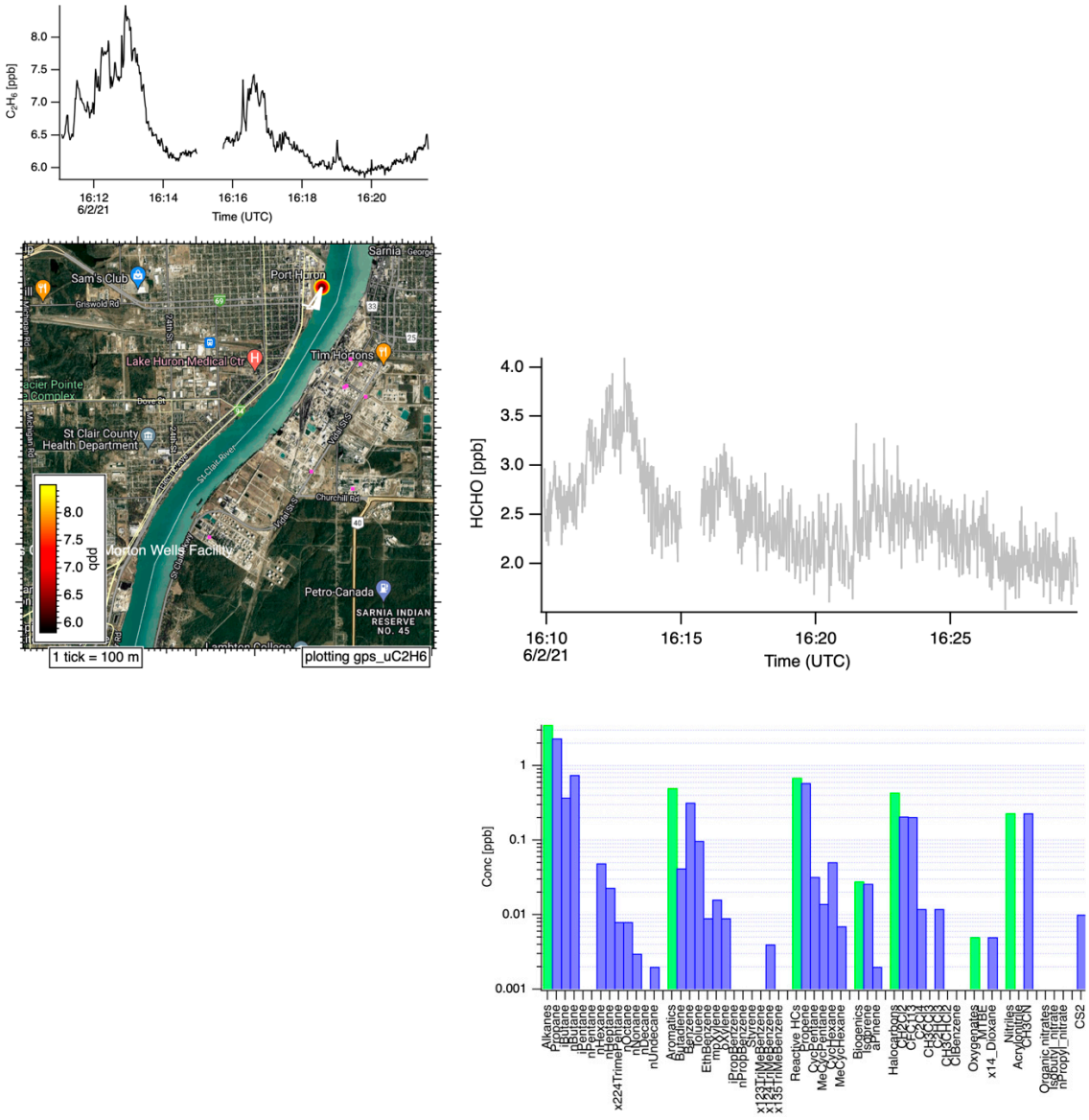

Figure S63. Stationary GC measurements showing 0.59 ppb propene enhancements. Satellite image source: Google Maps. Imagery ©2023 TerraMetrics.

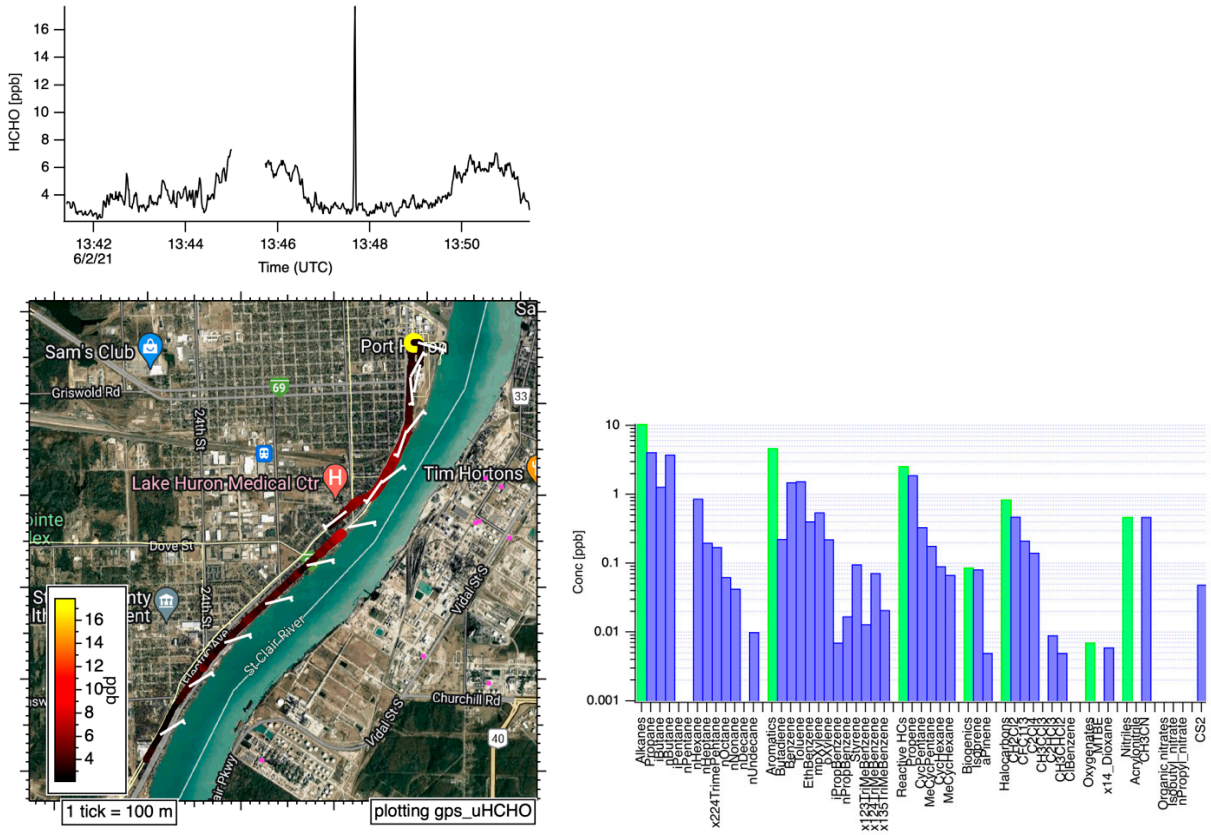

Figure S64. Mobile measurements including GC speciation downwind of Sarnia refineries showing 1.9 ppb propene enhancements. A brief exhaust spike can be seen around 13:47:30. Satellite image source: Google Maps. Imagery ©2023 TerraMetrics.

References

1. Herndon, S.C.; Jayne, J.T.; Zahniser, M.S.; Worsnop, D.R.; Knighton, B.; Alwine, E.; Lamb, B.K.; Zavala, M.; Nelson, D.D.; McManus, J.B.; et al. Characterization of urban pollutant emission fluxes and ambient concentration distributions using a mobile laboratory with rapid response instrumentation. *Faraday Discussions* **2005**, *130*, 327-339, doi:10.1039/b500411j.
2. Kolb, C.E.; Herndon, S.C.; McManus, J.B.; Shorter, J.H.; Zahniser, M.S.; Nelson, D.D.; Jayne, J.T.; Canagaratna, M.R.; Worsnop, D.R. Mobile Laboratory with Rapid Response Instruments for Real-time Measurements of Urban and Regional Trace Gas and Particulate Distributions and Emission Source Characteristics. *Environ. Sci. Technol.* **2004**, *38*, 5694-5703, doi:10.1021/es030718p.
3. Yacovitch, T.I.; Herndon, S.C.; Roscioli, J.R.; Floerchinger, C.; Knighton, W.B.; Kolb, C.E. Air Pollutant Mapping with a Mobile Laboratory During the BEE-TEX Field Study. *Environ. Health Insights* **2015**, 7-13, doi:10.4137/EHI.S15660.
4. McManus, J.B.; Zahniser, M.S.; Nelson, D.D.; Shorter, J.H.; Herndon, S.C.; Jervis, D.; Agnese, M.; McGovern, R.; Yacovitch, T.I.; Roscioli, J.R. Recent progress in laser-based trace gas instruments: performance and noise analysis. *Applied Physics B* **2015**, *119*, 203-218, doi:10.1007/s00340-015-6033-0.
5. Spinei, E.; Whitehill, A.; Fried, A.; Tiefengraber, M.; Knepp, T.N.; Herndon, S.; Herman, J.R.; Müller, M.; Abuhassan, N.; Cede, A.; et al. The first evaluation of formaldehyde column observations by improved Pandora spectrometers during the KORUS-AQ field study. *Atmos. Meas. Tech.* **2018**, *11*, 4943-4961, doi:10.5194/amt-11-4943-2018.
6. Yacovitch, T.I.; Herndon, S.C.; Roscioli, J.R.; Floerchinger, C.; McGovern, R.M.; Agnese, M.; Pétron, G.; Kofler, J.; Sweeney, C.; Karion, A.; et al. Demonstration of an Ethane Spectrometer for Methane Source Identification. *Environ. Sci. Technol.* **2014**, *48*, 8028-8034, doi:10.1021/es501475q.

7. Sekimoto, K.; Li, S.-M.; Yuan, B.; Koss, A.; Coggon, M.; Warneke, C.; de Gouw, J. Calculation of the sensitivity of proton-transfer-reaction mass spectrometry (PTR-MS) for organic trace gases using molecular properties. *International Journal of Mass Spectrometry* **2017**, *421*, 71-94, doi:10.1016/j.ijms.2017.04.006.
8. Pagonis, D.; Sekimoto, K.; de Gouw, J. A Library of Proton-Transfer Reactions of H3O+ Ions Used for Trace Gas Detection. *Journal of the American Society for Mass Spectrometry* **2019**, *30*, 1330-1335, doi:10.1021/jasms.8b06050.
9. Paatero, P.; Tapper, U. Positive Matrix Factorization - a Nonnegative Factor Model with Optimal Utilization of Error-Estimates of Data Values. *Environmetrics* **1994**, *5*, 111-126.
10. Paatero, P. A weighted non-negative least squares algorithm for three-way 'PARAFAC' factor analysis. *Chemometrics Intell. Lab. Syst.* **1997**, *38*, 223-242.
11. Lanz, V.A.; Alfarra, M.R.; Baltensperger, U.; Buchmann, B.; Hueglin, C.; Prévôt, A.S.H. Source apportionment of submicron organic aerosols at an urban site by factor analytical modelling of aerosol mass spectra. *Atmos. Chem. Phys.* **2007**, *7*, 1503-1522.
12. Ulbrich, I.M.; Canagaratna, M.R.; Zhang, Q.; Worsnop, D.R.; Jimenez, J.L. Interpretation of organic components from Positive Matrix Factorization of aerosol mass spectrometric data. *Atmos. Chem. Phys.* **2009**, *9*, 2891-2918.